WIS-71/35-Ph

Models for High Energy Photoproduction and Low-q^2 Electroproduction *)

Haim Harari

Department of Physics

The Weizmann Institute of Science

Rehovot, Israel

Rapporteur talk at the 5th International Symposium on Electron and Photon Interactions at High Energies, Cornell University, August 1971.

---

*) This work was performed in part under the sponsorship of the U.S. National Bureau of Standards

C O N T E N T S

1. Introduction

The study of the photoproduction of hadrons at multi-BeV energies has revealed striking similarities between these processes and the ordinary hadronic reactions. With only a few notable exceptions, the qualitative features of photon initiated hadronic processes resemble the observed properties of hadron collisions. In the previous conferences in these series, hadronic processes initiated by real photons attracted most of our attention[1],[2] simply because no other data were available. Since then, the measurements of the total photoabsorption of virtual space-like photons[3] (better known as inelastic electron scattering) have stimulated extensive experimental programs of studying the production of specific hadronic states by virtual photons[4] (a process better known as electroproduction). The goal is to reach a "continuous" experimental coverage and theoretical understanding of the physics of photon and electron reactions, from the $q^2=0$ limit of the real photon (which certainly shows hadron-like behaviour), through the low-q^2 region of virtual photons (which may exhibit hadron-like behaviour), to the large-q^2 "deep inelastic" region with its famous pointlike behaviour. In the three experimental review talks of Drs. Wiik[5], Wolf[6] and Berkelman[4], the impressive array of new data in high energy photoproduction and low-q^2 electroproduction was described. The present report is the theoretical counterpart of these three presentations. We shall try to discuss the theoretical highlights of the new data, emphasizing the intimate connection between hadron initiated reactions and (real and virtual) photon initiated processes. We shall touch only briefly upon the relation between the deep inelastic region and the low-q^2 electroproduction results. Most of the theoretical ideas which prevail in the so-called "scaling region"

are covered in the reports of Drs. Bjorken[7] and K. Wilson[8] to this conference, and we shall not discuss them here.

2. A Classification of Hadronic Two-Body Reactions

It would be appropriate to start our discussion of photo- and electroproduction by reminding ourselves of the basic types of mechanisms which are responsible for hadronic reactions[8]. Purely hadronic processes with two particles in the final state can be classified according to their dominant exchange mechanisms at high energies. We may distinguish between four classes of processes:

(a) Elastic and quasielastic reactions such as $\pi^{\pm}p \to \pi^{\pm}p$, $K^{\pm}p \to K^{\pm}p$, $pp \to pp$, $\bar{p}p \to \bar{p}p$, $\pi^{\pm}p \to A_1^{\pm}p$, $NN \to NN^*_{\frac{1}{2}}$, etc. The main features of these reactions at high energies include: (i) Approximately constant cross sections; (ii) Predominantly imaginary forward amplitudes; (iii) No quantum numbers are exchanged in the t-channel ($I_t=0$, $C_t=+1$); (iv) Natural parity exchange is dominant; (v) s-channel helicity is approximately conserved (for elastic but not for quasielastic processes). These features are characteristic to the diffractive (Pomeron-exchange) part of the amplitude. In addition, elastic and quasielastic processes have contributions from meson exchanges. The latter become smaller as the energy increases.

(b) Meson exchange reactions such as $\pi^-p \to \pi^0n$, $K^-p \to \pi^-\Sigma^+$, $pp \to n\Delta^{++}$, etc. Here, the exchange of a single non-exotic meson is dominant, possibly with absorption corrections corresponding to a meson-Pomeron cut in Regge language. The cross-sections for these reactions decrease with energy, usually with a power behaviour somewhere between s^{-1} and s^{-2}.

(c) Baryon exchange processes such as $\pi^+p \to p\pi^+$, $\pi^-p \to n\pi^0$, $K^+p \to pK^+$, $\pi^+d \to pp$, etc. A non-exotic baryon is exchanged, and the cross section falls

roughly like s^{-3}. Needless to say, the same meson-baryon reaction may involve meson exchange at forward angles and baryon exchange at backward angles, etc.

(d) Exotic exchange reactions such as $\pi^- p \to \pi^+ \Delta^-$, $K^- p \to \pi^+ \Sigma^-$, $K^- p \to p K^-$, etc. These presumably involve the exchange of a two-particle system, and the corresponding cross-sections decrease with energy much faster than those of the non-exotic exchange reactions.

These four classes represent the four basic types of reaction mechanisms in hadron physics, and it is convenient to refer to them in our discussion of photon-initiated reactions.

3. From Hadron Beams to Photon Beams - Classification of Photon-Induced Reactions.

Photoproduction cross-sections are typically smaller by a factor of 200 or so than the corresponding hadron cross sections. Electroproduction cross-sections are still smaller, since they involve one more factor of α than the corresponding processes with real photons. However, the gross features (s-dependence, t-dependence, resonances, dips, mechanisms, etc.) of all of these processes do not necessarily involve any conceptual differences. Except for the overall scale, we find great similarities between hadron, real photon, and virtual photon reactions.

Real photons have the technical advantage of enabling us to use polarized beams, a powerful tool for studying phenomenological models. They have the disadvantage of having a mixed isospin. Virtual photon beams, in addition to being polarized, have the fundamental advantage of enabling us to study cross-sections as a function of the mass of the external (virtual) particle. It is this property of electroproduction processes, which makes

them so attractive for studying the hadron structure. An even more exciting possibility is offered by the conjecture[10],[11],[7] that the effective radius which characterizes the interaction of a virtual photon with a hadron, changes as a function of the photon mass. If verified, such a property could yield an invaluable new tool for the study of hadronic production amplitudes. We shall return to this point several times in this report (sections 5, 15).

We shall now classify the various photo- and electroproduction processes with two-hadron final states, into the four classes of hadronic reactions mentioned above:

(a) "Elastic" photoproduction includes processes such as Compton scattering ($\gamma p \to \gamma p$) and vector meson (ρ^o, ω, ϕ) photoproduction and electroproduction. We know that[6]: (i) $\sigma_{tot}(\gamma N)$, $\frac{d\sigma}{dt}(\gamma N \to \gamma N)$, $\sigma(\gamma p \to \rho^o p)$, etc. are more or less constant (within 20% or so) above a few BeV[12]; (ii) At $t=0$, $\gamma p \to \gamma p$, $\gamma p \to \rho^o p$ and $\gamma p \to \phi p$ have predominantly imaginary amplitudes;[13] (iii) The dominant t-channel exchange has $I=0$, $C=+1$; (iv) Natural Parity exchange dominates[14]; (v) s-channel helicity is approximately conserved[15],[16]. Many experimental aspects of these reactions have been discussed in Wolf's talk[6]. We shall return to several of them later.

(b) Meson exchange photoproduction includes reactions such as $\gamma N \to \pi N$ and $eN \to e\pi N$, $\gamma N \to \pi\Delta$ and $eN \to e\pi\Delta$, etc. A large amount of new data have been presented in the reports of Wiik[5] and Berkelman[4], and we shall devote much of our discussion to these processes.

(c) Baryon exchange dominates the backward scattering region of all the above reactions. No new photoproduction ($q^2=0$) data have become available since the Liverpool conference;[17] and the systematics of the backward (baryon exchange) dips remains as puzzling as it was two years ago[2]. New

data on backward π^o-electroproduction were presented at the conference[4],[18]. As far as we can see, these new data pose no major new problems and solve no existing puzzles. We shall, therefore, not discuss these baryon exchange processes any further.

(d) Exotic reactions cannot occur, when we use a (real or virtual) photon beam. The process $\gamma+x \to y+z$ will always allow the (nonexotic) quantum numbers of particles x, y and z in the s, t and u channels, respectively. We may, however, study the strength of the contribution of exotic exchange amplitudes to non-exotic photoproduction cross sections. Such studies, for the reactions $\gamma N \to \pi^{\pm}\Delta$ and $\gamma N \to K^{+}\Sigma$, were reported at Liverpool[17],[2] and no new information has become available since then. Recent measurements of $\pi^{\pm}\Delta$ electroproduction[19],[4] are not at sufficiently high energy (or high accuracy) to lead to meaningful conclusions on this matter. We shall therefore not return to this topic in this report.

We are then left with "elastic" and "meson exchange" photoproduction and electroproduction, and the rest of this talk will be devoted to theoretical remarks concerning the recent developments in these processes.

4. A Short Guided Tour in the ν-q^2 Plane

Figure 1 shows the explored region of the ν-q^2 plane, where ν is the laboratory energy of the virtual photon and q^2 is its (spacelike) squared mass. The SLAC-MIT measurements[20],[3] of the total photoabsorption on proton and deuterium cover most of the shown region. Fixed W and ω lines are also shown ($W = \sqrt{s} = m^2 + q^2 + 2m\nu$; $\omega = \frac{2m\nu}{q^2}$; m = nucleon mass). The scaling region is roughly bounded by the W=2, q^2=1 and ω=12 lines[3]. Electroproduction experiments detecting specific hadronic final states were carried out only in a tiny region at low q^2. The figure shows the region for

which $ep \to e\pi^+ n$ data exist as well as the ν-q^2 values for which $ep \to ep^o p$ data were reported. It is evident that these data points are outside (or on the border of) the scaling region and it is not clear whether they have any bearing on the interesting puzzles of this region. On the other hand, the present data are in the transition region between $q^2=0$ photoproduction and the scaling region. It is presumably in this region, that the transition from the hadron-like quality of photoproduction amplitudes to the alleged point-like quality of deep inelastic electron scattering takes place. Both the SLAC-MIT experiment[20] and the compilation of data in the resonance region[21] indicate that, over most of the explored region of the ν-q^2 plane, the ratio σ_ℓ/σ_{tr} is very small, probably around 20%. We shall study below the composition of σ_ℓ in the low-q^2 region in terms of specific final states (section 13).

5. "Elastic" Photoproduction: Does the Interaction Radius Depend on q^2?

Assuming that forward elastic amplitudes are predominantly imaginary (as they seem to be), the elastic differential cross-section at small t-values enables us to determine the effective interaction radius for the diffractive component of elastic scattering. If $\frac{d\sigma}{dt} = Ce^{at}$, the impact parameter represantation of the (imaginary) diffractive amplitude obeys:

$$\text{Im } f(b) \propto e^{-\frac{b^2}{R^2}}$$

where the slope 'a' and the radius R are related by:

$$a = \frac{R^2}{4}$$

A measurement of the forward slope of a diffractive differential cross-section is therefore an indirect, but model independent measurement of the interaction

radius. The forward slope of $\frac{d\sigma}{dt}(\gamma p \to \gamma p)$ and $\frac{d\sigma}{dt}(\gamma p \to \rho^o p)$ is of the order $a \sim 8\ \text{BeV}^{-2}$, similar to typical slopes for purely hadronic elastic processes. This implies that, for $q^2=0$ photons, the photon-hadron interaction extends in space over a transverse distance which is comparable to the typical range of 1 fermi or so which is found in hadron collisions.

What is the interaction radius of a virtual spacelike photon with a squared mass q^2? Several interesting theoretical speculations on this subject have been proposed in the last few years[10],[11],[7], all of them pointing in the direction of a smaller radius as q^2 increases. In quantum electrodynamics the effective radius for producing lepton pairs in a potential, decreases when q^2 increases. A similar situation is expected in various versions of the parton model. A naive hand-waving explanation of this effect may run as follows: An incoming photon appears to a target proton as if it acquires a finite transverse size. This impression is created by the transverse recoil that the incident photon suffers when it produces parton pairs as a result of its interaction with the proton. The actual "spread" of the photon in the transverse direction depends on the number of pairs that it produces. When the photon is highly virtual, it lives only a very short time (because of the large energy mismatch) and succeeds in producing less pairs, thus suffering a smaller average transverse recoil. The virtual photon would then appear to have a smaller radius!

The simplest way to test this startling prediction is to measure the diffractive slope for electroproduction of ρ^o at different values of q^2. As q^2 increases, the slope (and the interaction radius) should decrease. Such experiments were performed at SLAC[22], Cornell[23] and DESY[24]. According to the SLAC experiment[22] the slope at $q^2=0.1$ is

$a = 7.4 \pm 0.8$ while at $q^2=0.5$ it is $a = 3.7 \pm 0.6$. A very dramatic effect, especially if we notice that a factor two in the slope leads to a difference of a full order of magnitude in one end of the measured t-region, if we hold the other end fixed! (figure 2). However, the Cornell experiment[23] shows a different picture (figure 3). The slope actually seems to increase considerably between $q^2=0.6$ and $q^2=1.2$! The Desy experiment[24] at $q^2=0.27$ is consistent with the $q^2=0.1$ measurement at SLAC and with the $q^2=0.3$ measurement at Cornell. The conclusion is, of course, that much more experimental work will have to be done before we know if the interaction radius of the virtual photon actually becomes smaller as q^2 increases. We have, however, a tantalizing hint that this may be the case, and no theorist would resist the temptation of speculating on the possible implications of such a behaviour. We shall return to speculate on this subject below (section 15).

6. "Elastic" Photoproduction - the Nondiffractive Component (A_2 and f^o Exchange)

Meson exchanges are always allowed in elastic processes, and their contributions can most easily be isolated by studying the deviations of elastic differential cross sections at finite energies from their assumed behaviour at the high energy limit. Thus, the difference $\sigma_t(\gamma p) - \sigma_t(\gamma n)$ is a measure of the $I=1$ (presumably A_2) exchange in forward Compton scattering while the deviation of the sum $\sigma_t(\gamma p) + \sigma_t(\gamma n)$ from a constant is a measure of the non-Pomeron $I=0$ exchange (presumably f^o). The best value for the relative strength of the f^o and A_2 contribution is[25],[6]

$$\frac{f^o}{A_2} = \frac{55.0 \pm 5.1}{12.3 \pm 2.3} = 4.5 \pm 1.3$$

This is consistent with the prediction $f^o/A_2 = 5$ of the quark model (or SU(3) with a pure F-coupling for the f^oNN vertex or duality diagrams).

Two other interesting features of the nondiffractive f^o and A_2 exchange in Compton scattering have not been studied yet. These are the dip in the elastic differential cross section and the crossover phenomenon. All hadronic elastic differential cross sections can be classified into two categories[26]: (i) pp and K^+p elastic differential cross sections show no structure for $t \leq 1$, they shrink with energy and they have exotic s-channel quantum numbers. (ii) $\bar{p}p$, K^-p, π^+p and π^-p elastic differential cross sections show dips between $t \sim -0.4$ and $t \sim -0.8$, the dips disappear as the energy increases, the differential cross sections do not shrink and they have non-exotic s-channel quantum numbers. These regularities, and particularly the correlation between the presence of dips and the s-channel quantum numbers have been explained[27] in a satisfactory way, using duality and absorption ideas. Since Compton scattering has nonexotic s-channel quantum numbers it should obviously behave like $\pi^{\pm}p$, K^-p or $\bar{p}p$ elastic scattering and show no shrinkage as well as a dip somewhere around $t \sim -0.6$ or so. The present data indicates no shrinkage (fig. 4), but the dip has not been observed, so far[28]. At what energies should we observe the dip? The relevant factor is the relative strength of the nondiffractive and diffractive contributions. In π^-p elastic scattering the dip is observed around $t \sim -0.7$ BeV for $p_\ell < 4$ BeV/c. At higher energies it disappears[29]. At 4 BeV/c the ratio between the nondiffractive and diffractive contributions to $\sigma_{tot}(\pi^-p)$ is approximately 1:2. In order to reach a similar ratio for $\sigma_{tot}(\gamma p)$ we have to go to $p_\ell \sim 2$ BeV. Consequently, the $t \sim -0.6$ dip should be observed for incident photon energies below 2 BeV (perhaps all

the way down to several hundreds MeV). A recent Desy experiment[28] (fig. 4) have yielded differential cross sections for Compton scattering which, unfortunately, extend beyond the expected dip region only for $E_\gamma > 5$ BeV. An extension of this experiment to lower energies and larger t-values should prove extremely interesting.

Another feature of hadronic elastic reactions is the famous crossover phenomenon. The differential cross sections for xp and $\bar{x}p$ elastic scattering, ($x = \pi^+, K^+, p$) cross each other somewhere around $t \sim -0.15$ BeV^2. This is explained by a zero in the imaginary part of the helicity nonflip nondiffractive amplitude. This zero is presumably related[27] to the zero of the function $J_0(r\sqrt{-t})$, for $r \sim 1$ fermi. A similar crossover is predicted for $\frac{d\sigma}{dt}(\gamma p \to \gamma p)$ and $\frac{d\sigma}{dt}(\gamma n \to \gamma n)$. In this case it is the A_2-exchange term which is supposed to have the form $J_0(r\sqrt{-t})$ while in the hadronic case the ρ- or ω-exchange terms are involved. We realize that it is extremely hard to locate the Compton scattering crossover in view of the difficulties involved in measuring Compton scattering on deuterium. However, since we already know from the total cross sections[25] that $\frac{d\sigma}{dt}(\gamma p \to \gamma p)_{0^\circ} > \frac{d\sigma}{dt}(\gamma n \to \gamma n)_{0^\circ}$, all one has to do in order to verify the existence of the crossover is to show that, say, at $t \sim -0.4$, $\frac{d\sigma}{dt}(\gamma n \to \gamma n) > \frac{d\sigma}{dt}(\gamma p \to \gamma p)$. It should be interesting to see if this prediction is verified.

7. "Elastic" photoproduction - the Nondiffractive Component (π exchange)

Diffraction scattering and single pion exchange are perhaps the two "oldest" reaction mechanisms in particle physics. Very rarely both of them appear in the same process. The only place where this seems to happen in

purely hadronic reactions is $NN \to NN$ where elastic scattering is mostly diffractive at high energies but is dominated by π-exchange at low energy. In πN and KN elastic scattering the pion cannot be exchanged, of course. It has been well known for several years that "elastic" photoproduction, in particular $\gamma p \to \omega p$, offers a unique opportunity to study π-exchange and Pomeron exchange in the same process. These two mechanisms are as different as they could possibly be: (i) $O\pi E$ gives $\sigma \propto s^{-2}$ while P-exchange gives $\sigma \propto$ Const; (ii) $O\pi E$ has $I_t=1$, P has $I_t=0$; (iii) $O\pi E$ is predominantly real, P-exchange is imaginary; (iv) $O\pi E$ mostly involves unnatural parity exchange while P-exchange has natural parity; (v) The $O\pi E$ contribution to $\gamma p \to \rho^o p$ is predicted by SU(3) to be nine times smaller than in $\gamma p \to \omega p$. The P-exchange contribution is nine times larger.

This impressive list of conflicting properties has been verified step by step during the last few years. The enhancement of $O\pi E$ relative to P-exchange in $\gamma p \to \omega p$ has been recognized long ago. The energy dependence of $\sigma(\gamma p \to \omega p)$ indeed seems to follow a $C_1 + C_2 s^{-2}$ behaviour, and the recent $E_\gamma = 9.3$ BeV data[30],[6] seems to show that this cross section has reached its constant value (within 20% or so). The same experiment shows a striking decline in the value of σ_U/σ_N, the ratio between the unnatural parity t-channel exchanges and the natural parity exchanges. For $E_\gamma = 9.3$ BeV one finds $\sigma_U/\sigma_N = 0.05 \pm 0.10$, while at 2.8 and 4.7 BeV $\sigma_U/\sigma_N \sim 1$. The picture may be slightly complicated by the contributions of A_2 and f^o exchanges[2],[6] but the gross features are a beautiful confirmation of the general notions of one-pion-exchange on one hand and Pomeron-exchange on the other hand.

8. The decay width $\Gamma(\rho \to \pi\gamma)$ - A new upper limit

The partial width for $\rho \to \pi\gamma$ is predicted by SU(3) to be:

$$\Gamma(\rho \to \pi\gamma) = \frac{1}{9}\,\Gamma(\omega \to \pi\gamma) \sim 0.12 \text{ MeV}$$

In other words

$$\frac{\Gamma(\rho \to \pi\gamma)}{\Gamma(\rho \to \pi\pi)} \sim 0.1\%$$

This small ratio, together with the experimental difficulty in distinguishing $\rho^{\pm} \to \pi^{\pm}\gamma$ from $\rho^{\pm} \to \pi^{\pm}\pi^{o}$ and $\rho^{o} \to \pi^{o}\gamma$ from $\omega \to \pi^{o}\gamma$ has made it very difficult to measure $\Gamma(\rho \to \pi\gamma)$ directly. Several indirect methods have been proposed in the past and, for a short while, it seemed[2] that $O\pi E$ analysis of different $\gamma p \to \rho^{-}\Delta^{++}$ and $\gamma n \to \rho^{-}p$ experiments led to satisfactory results. However, the energy dependence[31] of $\sigma(\gamma p \to \rho^{-}\Delta^{++})$ as well as certain features[32] of $\sigma(\gamma n \to \rho^{-}p)$ and the very low cross section for[33] $\gamma n \to \omega\Delta^{o}$ indicate that large contributions of other mechanisms (presumably ρ-exchange and A_2-exchange) are present in these reactions. This prevents us from using these reactions in order to determine $\Gamma(\rho \to \pi\gamma)$. On the other hand, the recent Laser beam measurements[34] of $\gamma p \to \rho^{o}p$ at $E_{\gamma} = 4.7$ BeV have yielded an extremely low upper limit for the contribution of unnatural parity exchanges to this reaction: $\sigma_{U}(\gamma p \to \rho^{o}p) \leq 0.3$ μb. Assuming that σ_{U} is entirely due to $O\pi E$ in both ρ^{o} and ω photoproduction we find:

$$\frac{\Gamma(\rho \to \pi\gamma)}{\Gamma(\omega \to \pi\gamma)} \sim \frac{\sigma_{U}(\gamma p \to \rho^{o}p)}{\sigma_{U}(\gamma p \to \omega\, p)} \leq \frac{0.3}{1.3}$$

Hence

$$\Gamma(\rho \to \pi\gamma) \leq 0.23 \text{ MeV}.$$

This upper limit, while still a factor of two above the predicted SU(3) value, is much more reliable than all previous limits . Measurements of $\gamma p \to \rho^- \Delta^{++}$ and $\gamma n \to \rho^- p$ with the polarized Laser beam should enable us to separate σ_U and σ_N for these reactions and to obtain even better determinations of $\Gamma(\rho \to \pi\gamma)$.

9. Compton Scattering - A J=0 pole?

We conclude our discussion of elastic photoproduction with a brief review of the only piece of evidence for a different behaviour for hadron reactions and photon reactions. Compton scattering off a proton must obey the famous Thomson limit theorem at low energies[35].

$$f_{\gamma p \to \gamma p}\ (\nu=0) \quad = \quad -\frac{\alpha}{m}$$

where f is the forward spin averaged Compton amplitude. The source of this theorem presumably has very little (if any) connection to the strong interactions of the proton and the theorem would certainly remain valid if someone "switches off" the strong interactions. From the point of view of a t-channel complex J-plane analysis, the nucleon Born term which is responsible for this limit would correspond to a J=0 fixed pole. Is this pole present at high energies?

More than two years ago, Creutz, Drell and Paschos[36] have proposed the possibility that the forward Compton amplitude contains a real constant at high energy and speculated that this constant may have the numerical value $(-\frac{\alpha}{m})$. In other words, they conjectured that the threshold value of the Thomson limit persists as a contribution to the real part of the amplitude at all energies.

There are two, essentially equivalent, ways of theoretically "detecting" such a constant. In both methods one parametrizes the imaginary part of the amplitude (i.e. the total cross section) at high energies as:

$$\text{Im } f(\nu) = C_P \nu + C_R \nu^{\frac{1}{2}}$$

where C_P and C_R are, respectively, the Pomeron and $(f_o + A_2)$ terms. The real part is then:

$$\text{Re } f(\nu) = -C_R \nu^{\frac{1}{2}} + C$$

where C is the real constant (i.e. the residue of the $J=0$ fixed pole). We are trying to find the value of C. The first method utilizes the finite energy sum rule:

$$-\frac{\alpha}{m} - \frac{1}{2\pi^2} \int_{\nu_o}^{N} \sigma_{tot}(\nu) d\nu = C - \frac{2C_P}{\pi} N - \frac{4C_R}{\pi} N^{\frac{1}{2}}$$

The other method uses the once-subtracted dispersion relation:

$$-C_R \nu^{\frac{1}{2}} + C = \text{Re } f(\nu) = -\frac{\alpha}{m} + \frac{\nu^2}{2\pi^2} \int_{\nu_o}^{\infty} \frac{d\nu'}{\nu'^2 - \nu^2} \sigma_{tot}(\nu')$$

In both cases σ_{tot} is taken from experiment and C_P and C_R are obtained by a fit to σ_{tot}. The constant C can then be computed. An analysis by Damashek and Gilman[37] indicated that the constant C is actually needed and that its numerical value is consistent with $-\frac{\alpha}{m}$. The results of their dispersion calculation are shown in figure 5. A confirmation of this result would necessitate more and better data for $\sigma_{tot}(\gamma p)$. A new measurement of σ_{tot} for the region $0 < E_\gamma < 4$ BeV was submitted to this conference by a group working at NINA.[38] It should prove extremely interesting to see whether these new total cross sections confirm the existence of a constant real term.

A similar problem arises for the same amplitude in the case of virtual Compton scattering, where $\sigma_{tot}(\gamma p)$ is measured in inelastic electron scattering experiments. In this case the analysis is, in principle, similar to the real photon case but the results depend in a very sensitive way on the assumptions used for the high ν behaviour of σ_{tot}. In particular, the sign of the residue of the fixed pole depends on the ν-value above which the form $\sigma_{tot} = C_o + C_1\nu^{-\frac{1}{2}}$ is assumed. The most naive calculation, assuming Regge behaviour at fairly low ν-values, actually gives for $q^2>1$ a fixed pole with an opposite sign to that found in the real photon case, but this type of calculation is highly unreliable[39]. We will return to this point in section 17.

If there is fixed J=0 pole in Compton scattering, does it also exist in $\gamma p \to \rho^o p$? Arguments for[40] and against such a possibility exist but none of them is very convincing and the situation is completely open.

10. Photoproduction of Charged Pions - Forward Spikes and Born Terms

At the SLAC(67) and Liverpool(69) conferences much attention was given[1),(2),(17),(41)] to the question of the sharp forward structures in the processes $\gamma p \to \pi^+ n$ and $\gamma p \to \pi^- \Delta^{++}$. Very little, if anything, has changed since then on this subject and we will not repeat here the discussion of the previous conferences. We are still in a situation where we know that the full Born terms for $\gamma p \to \pi^+ n$ (figure 6) and the "minimal" gauge invariant piece of the Born term for $\gamma p \to \pi^- \Delta^{++}$ (fig. 7) account for all the data at $|t| \leq m_\pi^2$, within 20% - 30%, and we still do not know why this is so. Several authors have reanalyzed this problem since 1969, with an emphasis on the $\gamma p \to \pi^- \Delta^{++}$ case which was not explored until then (except for the early work of Stichel and Scholz[42]). Dombey[43] have formulated a "rule"

which asserts that in charged π-photoproduction the $t \sim 0$ amplitudes are given at all energies by those terms in the low energy theorems which have a $1/E_\gamma^2$ energy dependence, while all other terms should be ignored. A similar rule was proposed by Campbell, Clark and Horn[44]. The rule works in the two cases of $\pi^+ n$ and $\pi^- \Delta^{++}$, but we do not really know why it works.

As we move from the $|t| < m_\pi^2$ region, the Born term fails miserably. Several years ago it was pointed out that the addition of the s and u-channel Δ-contributions provides an adequate explanation of the high energy data for larger t-values[45]. Recently, Barbour, Malone and Moorhouse[46] have extended this analysis by including many more N^* and Δ resonance in a dispersion calculation of the amplitudes for $\gamma p \to \pi^+ n$. They find an improved agreement with experiment. Their analysis have yielded the interesting feature that every single additional resonance contribution actually tends to decrease the cross section. (fig. 8). It would be interesting to try to understand this peculiar regularity which extends over a fairly large region in t.

11. Electroproduction of Charged Pions - The Born-Term Model

In view of the (mysterious) empirical success of the Born-term calculation for $\pi^\pm$-photoproduction at small t-values, it is only natural to speculate that a similar model could account for $\pi^\pm$-electroproduction at similar t-values and small photon masses. Several authors[47] have discussed the various aspects of such an approach. An interesting example of such a discussion is the work of Berends[47] who considered the diagrams of figure 9 as the dominant terms in small-t electroproduction of charged pions. His model includes corrections due to the Δ(1236) contributions, similar to those proposed earlier[45], in the photoproduction case. Among its other predictions, the Born-term model gives a large contribution of the longitudinal

component of the virtual photon. This contribution is expected to dominate the cross section for $e^- + p \to e^- + \pi^+ + n$.

A few words concerning the kinematics of pion electroproduction may be helpful at this point[4]. The measured differential cross section for final total hadronic mass $\sqrt{s}$, virtual photon mass $\sqrt{q^2}$ and squared nucleon momentum transfer t is given by an overall multiplicative factor (defining the "flux" of virtual photons) times an expression of the form:

$$\frac{d\sigma}{dt}(s,t,q^2) = \frac{d\sigma_{tr}}{dt}(s,t,q^2) + \varepsilon\frac{d\sigma_{\ell}}{dt}(s,t,q^2) + \varepsilon\cos 2\phi\ \frac{d\sigma_{pol}}{dt}(s,t,q^2) + \sqrt{\frac{\varepsilon(\varepsilon+1)}{2}}\cos\phi\ \frac{d\sigma_I}{dt}(s,t,q^2).$$

where $\frac{d\sigma_{tr}}{dt}$ is the total contribution of transversally polarized photons (analogous to $\frac{d\sigma_{\parallel}}{dt} + \frac{d\sigma_{\perp}}{dt}$ for $\gamma p \to \pi^+ n$ and to $\rho_{11}\frac{d\sigma}{dt}$ for $\pi N \to \rho N$); $\frac{d\sigma_{\ell}}{dt}$ is the total contribution of longitudinal photons (analogous to $\rho_{oo}\frac{d\sigma}{dt}$ for $\pi N \to \rho N$); $\frac{d\sigma_{pol}}{dt}$ is the contribution due to polarization effects of the transverse photons (analogous to $\frac{d\sigma_{\parallel}}{dt} - \frac{d\sigma_{\perp}}{dt}$ for $\gamma p \to \pi^+ n$ and to $\rho_{1,-1}\frac{d\sigma}{dt}$ for $\pi N \to \rho N$); $\frac{d\sigma_I}{dt}$ is the transverse-longitudinal interference term (analogous to $\rho_{10}\frac{d\sigma}{dt}$ for $\pi N \to \rho N$); ε defines the degree of longitudinal polarization of the virtual photon and ϕ is the angle between the electron scattering plane and the virtual photoproduction plane.

By performing coincidence measurements at different values of ε (i.e. different values of the electron scattering angle θ) and ϕ, but at the same values of s, t and q^2, the four $\frac{d\sigma}{dt}$ functions can be separated. Experiments at CEA[48], DESY[49] and NINA[50] have yielded cross sections for $e^- + p \to e^- + \pi^+ + n$ for several values of s, t and q^2 (mostly around $s \sim 5$ BeV^2, $|t| < 0.1$ BeV^2, $|q^2| < 1$ BeV^2). The experimental results have largely confirmed the predictions of the Born-term model, at least for small

t-values (say $|t| < 2m_\pi^2$). For larger t-values the predictions of the model are more sensitive to corrections due to Δ and N^* contributions, isoscalar photon contributions, etc. The agreement with experiment for such t-values is not spectacular. The longitudinal cross section σ_ℓ is definitely the dominant term over the region $|q^2| < 1$ BeV^2, as predicted by the model.

The dominance of σ_ℓ in the model follows from the importance of the t-channel pion pole and its coupling to the longitudinal photon. Since the q^2-dependence of the $\gamma\pi\pi$ vertex is unknown, we may use the general success of the Born-term description for the t-dependence, and deduce the pion form factor from the electroproduction data. Such a procedure is not totally unambiguous, as remarked in several recent papers on this subject[51],[52]. However, it seems clear that $F_\pi(q^2)$ is consistent with a single ρ-pole term as well as with the experimental isovector Dirac form factor of the nucleon, but it is larger than the $G_E(q^2)$ nucleon form factor (figure 10).

Similar Born-term models have been proposed[52] for other processes such as $e^- + N \to e^- + \pi^\pm + \Delta$. The early data on these processes[53] are not inconsistent with these models, but much more detailed experiments are needed for a better understanding of these reactions. Here, again, the longitudinal cross sections seems to be large. We shall return to these large σ_ℓ-values in section 13.

12. Electroproduction of Pions and Vector Meson Dominance

Very extensive literature exists on the subject of relating pion photoproduction cross sections to those for $\pi N \to \rho N$ and $\pi N \to \omega N$, via the vector dominance idea[54]. The first experimental results on π^+-electroproduction[48],[49],[50] offer a natural extension of this work

in several directions[55], all of which relate the cross sections for $V^oN \leftarrow \pi N$ to those for $\gamma N \rightarrow \pi N$ and $"\gamma"N \rightarrow \pi N$ (where $"\gamma"$ is a space-like virtual photon).

One type of extension of VMD involves the comparison of $\frac{d\sigma_{tr}}{dt}$ for $\pi^{\pm}$-electroproduction with $\frac{d\sigma}{dt}(\gamma p \rightarrow \pi^{+} n)$ and with $\rho_{11}\frac{d\sigma}{dt}(\gamma^{-} p \rightarrow V^o n)$. Such a study cannot shed any new light on questions such as the magnitude of the proportionality constant relating photon reactions to vector meson reactions. It may, however, test the q^2-dependence of the transverse cross section, and compare it with the simple ρ-propagator form implied by VDM. It is almost certain that such a test will fail at large q^2-values, in view of the repeated failures of VMD for such values in elastic and deep inelastic ep scattering[56]. However, at small values of q^2 (say, below 1 BeV^2) such an approximation may be valid. The data for $\frac{d\sigma_{tr}}{dt}$ are not very accurate, but they are, at present, not inconsistent[55] with the q^2-dependence predicted by VMD.

A totally different class of VMD tests involves the comparison between the longitudinal cross sections in the timelike and spacelike regions. The longitudinal component of the vector meson cross section $\rho_{oo}\frac{d\sigma}{dt}(\pi^{-} p \rightarrow V^o n)$, can be compared with real photoproduction data only by using additional assumptions concerning the smoothness of a specific set of invariant photo-production amplitudes[57]. The comparison of $\rho_{oo}\frac{d\sigma}{dt}(\pi^{-} p \rightarrow V^o n)$ with $\frac{d\sigma_{\ell}}{dt}(\,"\gamma"p \rightarrow \pi^{+} n)$ is more direct, although a kinematic factor of q^2 has to be inserted in order to guarantee the vanishing of ρ_{oo} (or σ_{ℓ}) for $q^2=0$. Several authors have performed such comparisons[55] and the details vary. The overall picture is, however, that within 20% - 40%, agreement can be achieved. A typical example is shown in figure 11 where the $q^2=0.75$ data seems to indicate even better agreement than the $q^2=0.26$ data (surely an accident!).

13. An Interesting Exercise Concerning Longitudinal Electroproduction Cross Sections

The single-arm inelastic electron scattering experiments have indicated that the total photoabsorption cross section for virtual photons is dominated by the contributions of the transverse photon[20]. The ratio σ_ℓ/σ_{tr} is found to be around 20% or so, and consistent with zero both in the so called "deep inelastic region"[20] and throughout the resonance region[21]. On the other hand, the specific channels $e^-+p \to e^-+\pi^++n$, $e^-+p \to e^-+\pi^++\Delta^o$ and $e^-+p \to e^-+\pi^-+\Delta^{++}$ show relatively large contributions of the longitudinal photon[48],[49]. It is clear that no contradiction is involved here[52], since these three channels account only for a small fraction of the full photoabsorption cross section. Nevertheless, it is interesting to compare the longitudinal and transverse parts of these cross sections for specific final states with the longitudinal and transverse parts of the total cross section.

Since most of the $\pi^\pm$-electroproduction data are at $W=\sqrt{s}=2.3$ BeV, we shall first discuss the situation in this particular energy region. For real photons at $W=2.3$, $\sigma_{total}(\gamma p) \sim 140$ μb, $\sigma(\gamma p \to \pi^+ n) \sim 4$ μb, $\sigma(\gamma p \to \pi^-\Delta^{++}) \sim 6$ μb, $\sigma(\gamma p \to \pi^+\Delta^o) \sim 2$ μb. These estimates are based on the existing differential cross sections around this energy value[58]. The three processes under consideration account for approximately 9% of the total cross section. In the virtual photon case, the transverse component σ_{tr} probably follows a similar pattern, since for $|q^2| < 1$ BeV^2 the q^2-dependence of the total transverse cross section is more or less the same as the q^2-dependence of the σ_{tr} parts for $e^-+p \to e^-+\pi^++n$, $e^-+\pi^++\Delta^o$, $e^-+\pi^-+\Delta^{++}$.

An entirely different picture emerges for the longitudinal cross section. Let us consider a specific q^2-value, say $q^2=0.8$. The compilation of Brasse et al.[21] indicates that for $W=2$, $q^2=0.5$, $\sigma_{tr}+\varepsilon\sigma_\ell \sim 90$ μb. For $W=2$, $q^2=1$, $\sigma_{tr}+\varepsilon\sigma_\ell \sim 60$ μb. In both cases the ε-dependence is negligible. These authors find that over the entire $W\leq 2$ region $\sigma_\ell/\sigma_{tr} \leq 20\%$. Interpolating between the q^2-values and extrapolating to $W=2.3$ we conclude that for $W=2.3$, $q^2=0.8$, $\sigma_\ell \leq 12$ μb. This seems to be in reasonable agreement with the SLAC-MIT data[20], although in their case the value of σ_ℓ/σ_{tr} was deduced only for larger q^2-values. It is difficult to determine the longitudinal cross section for our three single channels, since most of the data are at relatively small t-values and the full cross sections involve an integration over all t. It is possible, however, to estimate these cross sections within a factor of two or so from the existing measurements and mild theoretical assumptions such as assuming that the slope in t of $\frac{d\sigma_\ell}{dt}(\bar{e}p \to e\pi^+ n)$ is, within a factor of two, the same as the slope of $\rho_{oo}\frac{d\sigma}{dt}(\pi^- p \to \rho^o n)$, etc. With such assumptions, we learn that at $W=2.3$, $q^2=0.8$: $\sigma_\ell(e^-+p \to e^-+\pi^++n) \sim 2 - 5$ μb; $\sigma_\ell(e^-+p \to e^-+\pi^-+\Delta^{++}) \sim 3 - 6$ μb; $\sigma_\ell(e^-+p \to e^-+\pi^++\Delta^o) \sim 1 - 4$ μb. The sum of these three channels is therefore at least 50%, possibly more than 100% (?!) of the estimated total longitudinal cross section at the same point!

Every single numerical estimate in our previous discussion should be regarded as crude and highly speculative. The overall conclusion is, however, unavoidable: Most, if not all, of the longitudinal total virtual photoabsorption cross section is given by the $\pi^+ n$ and $\pi^\pm\Delta$ final states.

This result immediately leads to several remarks:

(i) The ratio σ_ℓ/σ_{tr} is not zero. While the SLAC-MIT measurements[20] and the DESY compilation[21] indicate that σ_ℓ/σ_{tr} is consistent

with zero, the three ($\pi^+ n$ and $\pi^\pm \Delta$) channels are sufficient to establish a lower limit for this ratio. This lower limit, for $W=2.3$ and $q^2 < 1$ BeV^2, is not much smaller than the upper limit of the single arm experiments.

(ii) In parton models, σ_ℓ/σ_{tr} is predicted to vanish for spin-½ partons while σ_{tr}/σ_ℓ vanishes for spin 0 partons. The observed small value of σ_ℓ/σ_{tr} is usually considered as evidence for spin-½ partons. It is interesting that we find that most (or all) of the small longitudinal cross section is actually dominated by single $\pi^\pm$ production, presumably through diagrams in which the photon couples directly to the pion. It is clear that the pion is not a parton in this case (since the deduced form factor $F_\pi(q^2)$ is not point-like) and it should be extremely interesting to see whether at large ("deep" inelastic) values of q^2 a similar situation occurs.

(iii) The three channels discussed here disappear rapidly as the energy increases ($\sigma \propto 1/s^2$). On the other hand, higher N^*-states can be excited and eventually one may consider the so-called "Drell process" for virtual photons (figure 12). The cross section for this process is presumably constant in energy. If σ_ℓ/σ_{tr} is found to be constant in energy, it would be interesting to see whether σ_ℓ can be accounted for by the mechanism of figure 12 at all energies. If σ_ℓ/σ_{tr} decreases with energy, σ_ℓ might be related only to a few N^* and Δ states which are produced in the final state together with the charged pion.

It is clear that the present data are not sufficiently accurate for a detailed analysis of these questions. Better determinations of σ_ℓ/σ_{tr} as well as large t measurements of $\pi^\pm$-electroproduction would be very helpful.

14. Photoproduction of π^o and η, dips and all that

At the time of the Liverpool conference we have devoted much attention[2] to the erratic behaviour of dips in differential cross sections for processes such as $\gamma p \to \pi^o p$, ηp, $\pi^+ n$ and $\pi N \to \rho N, \omega N$ etc. Since then, substantial progress has been made in understanding the regularities of these dips[59],[60] and their most attractive description is based on a model involving dominant contributions from the most peripheral partial waves. These contributions presumably account for the imaginary part of the amplitude while the real part is given in some cases by the asymptotic relation between the energy dependence and the phase and in other cases cannot be predicted in any simple way.

The favorite models of several years ago (the "Michigan" and "Argonne" models) are clearly inadequate[59],[60] and the present picture indicates that: (i) At least in some cases very strong absorption corrections are needed; (ii) There is no reason to abandon ghost killing zeroes and nonsense zeroes in the Regge pole contribution (before absorption is applied); (iii) The relative strength of the pole terms and cut terms vary dramatically between different helicity amplitudes, even in the same process. (iv) The phase relation between the real and imaginary parts of the same amplitude is simple in some cases and not understood at all in others.

In spite of the fact that all the circumstancial evidence seems to favour the correlation between dips and geometrical effects, we still lack a decisive test of this issue. The confusion stems from the following peculiar situation.

One group of models (the "nonsense models") relates dips at $|t| \sim 0.5$ to nonsense points of the vector and tensor trajectories ($\alpha(t) \sim 0.5 + t$). Another group of models (the "radius models") relates the same dips to the

zero of the Bessel function $J_1(r\sqrt{-t})$ for $r \sim 1$ fermi. This is the predicted t-dependence for a single-helicity-flip amplitude dominated by its most peripheral ($b \sim 1$ fermi) partial waves. Since all the observed $|t| \sim 0.5$ dips (in $\pi^- p \to \pi^0 n$, $\pi N \to \pi\Delta$, $\gamma p \to \pi^0 p$ and $\pi^\pm p \to \rho^\pm p$) occur in processes involving vector meson exchange, and since in all of these processes the single helicity-flip dominates, it is hard to distinguish between the two types of models in a direct way.

A unique way of settling this point may be offered by an electroproduction experiment. We discuss it in the next section.

15. Electroproduction of π^0 - A Crucial Test of Dip Mechanisms

The simplest way to resolve the dispute between the "nonsense models" and the "radius models" (see previous section) would be to "move" the zeroes of $\alpha(t) = 0.5 + t$ and of $J_1(r\sqrt{-t})$ away from each other. This can be done either by changing the parameters of the exchanged vector meson (we do not know how to accomplish this) or by changing the effective interaction radius of the collision. In section 5, we have discussed the intriguing possibility that the interaction radius for a virtual photon and a hadron may depend on the photon mass. We have mentioned that the data may already be hinting in this direction, although no firm conclusions can be drawn. If, however, the interaction radius associated with the virtual photon indeed decreases when the photon mass increases, it may provide us with a simple and elegant way[61] of distinguishing between the dip mechanisms suggested by the "nonsense models" and by the "radius models". For the sake of the argument, let us suppose that between $q^2=0$ and $q^2=0.5$ the value of r^2 decreases by a factor two, as suggested by the SLAC experiment[22].

(This is by no means clear, as it is not confirmed by the Cornell experiment[23]. We use it only as an illustration). This would change the argument of the expression $J_1(r\sqrt{-t})$ without changing $\alpha(t) \sim 0.5 + t$. All we have to do is to measure the transverse photon contribution to π^o-electroproduction and to see whether the $|t| \sim 0.5$ dip moves as a function of the virtual photon mass. If r^2 indeed changes by a factor of 2, the dip position should shift according to the "radius models" from $|t| \sim 0.5$ to somewhere between $|t| \sim 0.7$ and $|t| \sim 1$, depending on the details of the model[61]. According to the "nonsense models" the dip should remain around $|t| \sim 0.5$ regardless of the value of q^2.

We must emphasize that this test is relevant and crucial only if the diffractive slope for ρ^o-electroproduction is really found to change with q^2. If it remains independent of q^2, we return to the situation of a fixed interaction radius and the π^o-electroproduction experiment will not make us any wiser. We feel that the π^o experiment, subject to a verification of the changing slope for ρ^o-electroproduction, may be an extremely interesting experiment and we hope that by the time of the 1973 conference this issue will be settled.

16. Some Trivial, but Strange, Consequences of Varying the Photon Mass

The option of varying the external mass in a hadronic collision and the spacelike character of this mass are unique to electron scattering. The kinematics of such reactions lead to several trivial, but strange, consequences especially with respect to geometrical descriptions of hadronic reactions. The normal relation between ℓ, the relative orbital angular momentum and r, the interaction radius, is given by $\ell \sim p_{c.m.} r$ (we assume, for simplicity, $\ell >> j_1, j_2$ where j_1, j_2 are the spins of the colliding particles). Figure 13

shows, on a Chew-Frautschi plot, the ℓ-values corresponding to impact parameters smaller than a certain radius (r=1 fermi) for a real photon-proton collision. The "allowed" range of ℓ-values is bounded by a curve which, asymptotically, approaches a parabola of the form $\ell \sim \frac{1}{2} r\sqrt{s}$. The entire "allowed" region lies below the leading N and Δ trajectories and is presumably densely populated by resonances.

When the photon acquires a spacelike mass $\sqrt{q^2}$, the curve described by the relation $\ell \sim p_{c.m.} r$ moves in the ℓ-s plane (the Chew-Frautschi plot) and "invades" the region above the leading N and Δ trajectories (figure 13). For instance, when $s=W^2=5$ BeV^2 and r=1 fermi the maximal ℓ-value is around 4 or 5 for $q^2=0$, and 7 or 8 for $q^2=2$ BeV^2. The leading nucleon or Δ trajectory reaches $\ell \sim 5$ for this s-value. What happens to the $\ell=6,7,8$ partial wave amplitudes when we scatter a $q^2=2$ photon on a proton at s=5? Do they vanish, effectively yielding a smaller interaction radius? Do they contribute to the scattering? If they do, is the contribution due to new resonances which are not excited in ordinary γp or πp collisions? Is it due to nonresonant "background"? Is the simple $\ell \sim p_{c.m.} r$ relation valid and relevant under such circumstances?

All of these questions have to be answered by any detailed model for electroproduction processes. They are particularly crucial in resonance models and in geometrical models, and they certainly deserve much theoretical attention. In addition to the kinematical effect discussed here, the radius r may vary with q^2 (see sections 5, 15), thus complicating the issue even further.

17. The Relation Between Real Photoproduction and the Scaling Region

In photoproduction processes involving real photons, we have a fairly good "feeling" for the kind of physics that we may expect at any given energy region. Thus, below ν=2 BeV the large resonances dominate; around 2-3 BeV

we reach a transition region where the prominent resonances are not so easy to detect, and the simple Reggeistic energy dependence starts to be felt at higher energies, the energy dependence is represented by a simple power behaviour where the specific power is related to the exchanged quantum numbers in the t-channel. A similar behaviour is observed in purely hadronic processes such as $\pi^{\pm}p$ scattering.

When we study photoproduction by virtual photons we would normally expect a resonance region, a transition region and a "Regge" region. However, in the scaling region the relevant variable is presumably the dimensionless quantity $\omega = \frac{2m\nu}{q^2}$. At low ω we are still at some threshold region with resonance contributions, etc. At sufficiently high ω we presumably reach a simple (Reggeistic?) power behaviour of the total cross section (or W_1, νW_2, etc.). Since ω is dimensionless, it is not a priori clear, for instance, at what ω-values we should expect the Reggeistic domain to begin. Is the physics of virtual photoproduction at, say, $\omega \sim 10$ similar somehow to the physics of real photoproduction at ν=10 BeV? ν=1 BeV? ν=200 MeV? We realize that we are not asking here a well defined question, but in one sense or the other the "asymptotic high ω region" has to be identified, and we ask whether we are already in it when we perform measurements at $\omega \sim 10$ or whether, perhaps, we have to go to much higher ω-values before ideas on diffraction, Reggeism, etc. may become applicable.

At least three different groups of authors, using different motivations, have recently expressed the opinion that the ω-values which are in some sense analogous to ν-values of a few BeV in real photoproduction, are actually very large, possibly of the order of 50-100.

Rittenberg and Rubinstein[62] have tried a phenomenological extension of the scaling variable ω into the q^2=0 region. They found that a variable

of the form $\omega_W = \frac{2m\nu + A}{q^2 + B}$ can be used in connecting experimental values of the W_1 structure function between $q^2=0$ (real photoproduction) and the scaling region. A recent DESY fit[63] seems to prefer the values $A \sim 1.4$ BeV^2, $B \sim 0.4$ BeV^2. Lines of fixed ω_W on the ν-q^2 plane (fig. 14) show that ω-values between 20 and 50 are related to ν-values around 3 BeV for real photoproduction. In this sense one would perhaps expect the Regge domain to start only above $\omega \sim 50$ or so.

Similar conclusions concerning the high ω-values needed for reaching "high energies" were expressed by Gilman[64] on the basis of speculations regarding the relative importance of the diffractive and nondiffractive components of νW_2 and by Close and Gunion[65] on the basis of assuming that the $J=0$ fixed pole in νW_2 has the same sign as the similar pole in the forward Compton amplitude for real photons (see section 9). None of these arguments is very rigorous , but the remarks of these three groups of authors at least raise an interesting question. It is clear that careful measurements of low q^2 cross sections will teach us much more on the relation between real photoproduction and the scaling region, and will help us to define the so-called asymptotic large-ω region where diffraction and/or Reggeizm apply.

18. Concluding Remarks

We regard the new data on low-q^2 electroproduction of specific final states as an exciting beginning of a new field of investigation in hadron physics. The possibility of studying the nature of hadronic processes as a function of the masses of the colliding particles is particularly interesting. The possible dependence of the interaction radius on the photon mass, if verified, will certainly create a new

powerful tool for phenomenological analysis. A coverage of the entire q^2 range between zero and the scaling region may enable us to find the connection between ordinary hadron phenomenology (presumably applicable at $q^2=0$) and the "deep inelastic" phenomenology of partons and light cones (presumably applicable at relatively large-q^2). Experiments such as ρ^o, π^o and $\pi^\pm$ electroproduction should be improved, repeated and extended to new s, t and q^2 regions. At the same time we continue to learn from the real photoproduction data, and several unexplored processes such as intermediate t, low energy, Compton scattering or large t, π-photoproduction are still to be measured.

A theoretical field of investigation which will have to be extensively developed in the near future is the analysis of the low energy-high energy relations for electroproduction amplitudes. It is clear that fixed-q^2 and variable-q^2 FESR's for electroproduction may teach us a great deal. It is even possible that some of the answers to the many questions that we have raised in this report are buried somewhere in the existing electroproduction data in the resonance region. A careful theoretical evaluation of these data may be extremely fruitful.

I would like to express my thanks to my experimental and theoretical colleagues at SLAC for their help and advice during the preparation of this review.

References

1. H. Harari, Rapporteur talk, 3rd International Symposium on Electron and Photon Interactions at High Energies, Stanford, California, 1967, p. 337.
2. H. Harari, Rapporteur talk, 4th International Symposium on Electron and Photon Interactions at High Energies, Liverpool, 1969, p. 107.
3. H. Kendall, Rapporteur talk, these Proceedings.
4. K. Berkelman, Rapporteur talk, these Proceedings.
5. B. Wiik, Rapporteur talk, these Proceedings.
6. G. Wolf, Rapporteur talk, these Proceedings.
7. J.D. Bjorken, Rapporteur talk, these Proceedings.
8. K. Wilson, Rapporteur talk, these Proceedings.
9. For a detailed discussion of photoproduction processes from this point of view see, e.g., H. Harari, Proceedings of the Scottish Universities Summer-school, 1970, Academic Press.
10. H. Cheng and T.T. Wu, Phys. Rev. 183, 1324 (1969).
11. J.D. Bjorken, J. Kogut and D. Soper, Phys. Rev. D1, 1382 (1971); J.D. Bjorken, Proceedings of the Tel-Aviv Conference on Duality and Symmetry in Hadron Physics, 1971.
12. For a review see, e.g., D.W.G.S. Leith, Proceedings of the Scottish Universities Summerschool, 1970, Academic Press.
13. A.M. Boyarski et al., Phys. Rev. Letters 26, 1600 (1971); R.L. Anderson et al., Phys. Rev. Letters 25, 1218 (1970); H. Alvensleben et al., Phys. Rev. Letters 27, 444 (1971), 25, 1377 (1970).
14. J. Ballam et al., SLAC preprint, submitted to this symposium.
15. J. Ballam et al., Phys. Rev. Letters 24, 960 (1970).
16. F.J. Gilman, J. Pumplin, A. Schwimmer and L. Stodolsky, Phys. Letters 31B, 387 (1970).

17. K. Lubelsmeyer, Rapporteur talk, 4th International Symposium on Electron and Photon Interactions at High Energies, Liverpool, 1969, p. 45.

18. C.N. Brown et al., Harvard preprint, submitted to this symposium; C. Driver et al., DESY preprint, submitted to this symposium.

19. C.N. Brown et al., Harvard preprint, submitted to this symposium.

20. E.D. Bloom et al., SLAC-PUB-796; SLAC-PUB-805; report to the Kiev Conference 1970; SLAC preprint, submitted to this symposium; R.E. Taylor, invited talk, 4th International Symposium on Electron and Photon Interactions at High Energies, 1969, p. 251.

21. F.W. Brasse et al., DESY preprint 71/19, submitted to this symposium.

22. E.D. Bloom et al., SLAC-PUB-955, submitted to this symposium.

23. D.E. Andrews et al., Cornell preprint CLNS-169, submitted to this symposium.

24. C. Driver et al., DESY preprint, submitted to shis symposium.

25. D.O. Caldwell et al., Phys. Rev. Letters 25, 609 (1970).

26. See, e.g., D.R.O. Morrison, Rapporteur talk, International Conference on Elementary Particle Physics, Lund, 1969.

27. H. Harari, Annals of Physics (N.Y.), 63, 432 (1971).

28. G. Buschhorn et al., DESY preprint, submitted to this symposium.

29. See, e.g., G. Giacomelli et al., CERN-HERA-69-1.

30. J. Ballam et al., SLAC preprint, submitted to this symposium.

31. J. Ballam et al., Phys. Rev. Letters 26, 995 (1971).

32. P. Benz et al., DESY preprint, submitted to this symposium.

33. Y. Eisenberg et al., Phys. Rev. Letters 25, 764 (1970).

34. J. Ballam et al., SLAC preprint, submitted to this symsposium.

35. M. Gell-Mann and M.L. Goldberger, Phys. Rev. 96, 1433 (1954); F.E. Low, Phys. Rev. 96, 1428 (154).

36. M.J. Creutz, S.D. Drell and E. Paschos, Phys. Rev. 178, 2300 (1969).

37. M. Damashek and F.J. Gilman, Phys. Rev. D1, 1319 (1970).

38. T.A. Armstrong et al, Glasgow-Sheffield preprint, submitted to this symposium.

39. J.M. Cornwall, D. Carrigan and R.E. Norton, Phys. Rev. Letters 24, 1141 (1970); S.R. Choudhury and R. Rajaraman, Phys. Rev. D2, 2728 (1970); M. Elitzur, Phys. Rev. D3, 2166 (1971); F.E. Close and J.F. Gumion, SLAC-PUB-892, to be published.

40. R.A. Brandt et al., NYU preprint, submitted to this conference.

41. B. Richter, Rapporteur talk, 3rd International Symposium on Electron and Photon Interactions at High Energies, Stanford, California 1967, p. 309.

42. P. Stichel and M. Scholz, Nuovo Cimento 34, 1381 (1964).

43. N. Dombey, Phys. Letters 30B, 646 (1969); D.J. Broadhurst, N. Dombey and B.J. Read, Phys. Letters 34B, 95 (1971).

44. J.A. Campbell, R.B. Clark and D. Horn, Phys. Rev. D2, 217 (1970).

45. J. Engels, G. Schwiderski and W. Schmidt, Phys. Rev. 166, 1343 (1968).

46. I. Barbour, W. Malone and R.G. Moorhouse, Berkeley preprint, UCRL-20635, submitted to this symposium.

47. See, e.g., F.A. Berends, Phys. Rev. D1, 2590 (1970).

48. C.N. Brown et al., Phys. Rev. Letters 26, 987 (1971).

49. C. Driver et al., Phys. Letters 35B, 77 (1971).

50. P.S. Kummer et al., Lettere al Nuovo Cimento 1, 1026 (1971).

51. W. Schmidt, DESY preprint 71/22, submitted to this symposium; R.C.E. Devenish and D.H. Lyth, Lancaster preprint, submitted to this symposium; J.D. Sullivan, Phys. Letters 33B, 179 (1971).

52. F.A. Berends and R. Gastmans, Harvard-MIT preprint, submitted to this symposium.

53. C.N. Brown et al., Harvard preprint, submitted to this symposium; C. Driver et al., DESY preprint 71/25, submitted to this symposium.

54. See, e.g., K. Lubelsmeyer, referemce 17; D. Schildknecht, DESY preprint, 1970; A. Dar, Technion preprint 1970.

55. H. Fraas and D. Schildknecht, Phys. Letters 35B, 72 (1971); F.A. Berends and R. Gastmans, Phys. Rev. Letters 27, 124 (1971); R. Mamveiler and W. Schmidt, Phys. Rev. D3, 2752 (1971); A. Fraas and D. Schildknecht, DESY preprint, submitted to this symposium.

56. See, e.g., R.E. Taylor, invited talk, 4th International Symposium on Electron and Photon Interactions at High Energies, Liverpool, 1969, p. 251.

57. C.F. Cho and J.J. Sakurai, Phys. Letters 30B, 119 (1969); Phys. Rev. D2, 517 (1970).

58. See, e.g., P. Joos, DESY-HERA-70-1.

59. See, e.g., H. Harari, SLAC-PUB-914, to be published in the Proceedings of the Tel-Aviv Conference on Duality and Symmetry in Hadron Physics, April, 1971.

60. See, e.g., R.J.N. Phillips, Rapporteur talk at the Amsterdam Conference, July 1971 (Rutherford Laboratory preprint).

61. H. Harari, SLAC-PUB-953, to be published.

62. V. Rittenberg and H.R. Rubinstein, Phys. Letters 35B, 50 (1971).

63. J. Moritz et al., submitted to this symposium.

64. F.J. Gilman, Proceedings of the Tel-Aviv Conference on Duality and Symmetry in Hadron Physics, April, 1971.

65. F.E. Close and J.F. Gunion, SLAC-PUB-892, to be published.

Figure Captions

Figure 1. The ν-q^2 plane. Fixed W and fixed ω lines are shown as well as the "scaling region". The values for which π^+ and ρ^o electroproduction data are available are also indicated.

Figure 2. The diffraction peak for ρ^o electroproduction (from reference 22).

Figure 3. The diffraction peak for ρ^o electroproduction (from reference 23).

Figure 4. Differential cross sections for Compton scattering (from referemce 28).

Figure 5. The real part of the forward $\gamma p \to \gamma p$ amplitude as a function of energy, computed from a once subtracted dispersion relation (solid line) and from the expression $-C_R \nu^{\frac{1}{2}}$ (dashed line). The difference between the two measures the real constant (J=0 fixed pole). The value of $-\frac{\alpha}{m}$ in these units is -3. The labels A, B, A&B denote different fits to the high energy total cross sections (from reference 37).

Figure 6. Born diagrams for $\gamma p \to \pi^+ n$

Figure 7. Born diagrams for $\gamma N \to \pi^{\pm} \Delta$

Figure 8. Dispersion calculation of $\frac{d\sigma}{dt}(\gamma N \to \pi^{\pm} N)$ and its dependence on the contributions of the various N^* and Δ resonance (from reference 46).

Figure 9. Electric Born diagrams for $e^- p \to e^- \pi^+ n$.

Figure 10. The pion form factor, as deduced from a Born term model for $e^- p \to e^- \pi^+ n$. The data used are from references 48 and 49. (The figure is taken from reference 52).

Figure 11. Comparison of π^+-electroproduction data with $\pi^- p \to \rho^o n$ data, using vector meson dominance. (From Fraas and Schildknecht, reference 55).

Figure 12. The "Drell process" for virtual photoproduction of charged pions.

Figure 13. A Chew-Frautschi plot for γ-N scattering. The curves $\ell = P_{c.m.} r$ are shown for different values of the spacelike photon squared mass $-q^2$.

Figure 14. Fixed-ω lines and fixed ω_W-lines in the ν-q^2 plane.

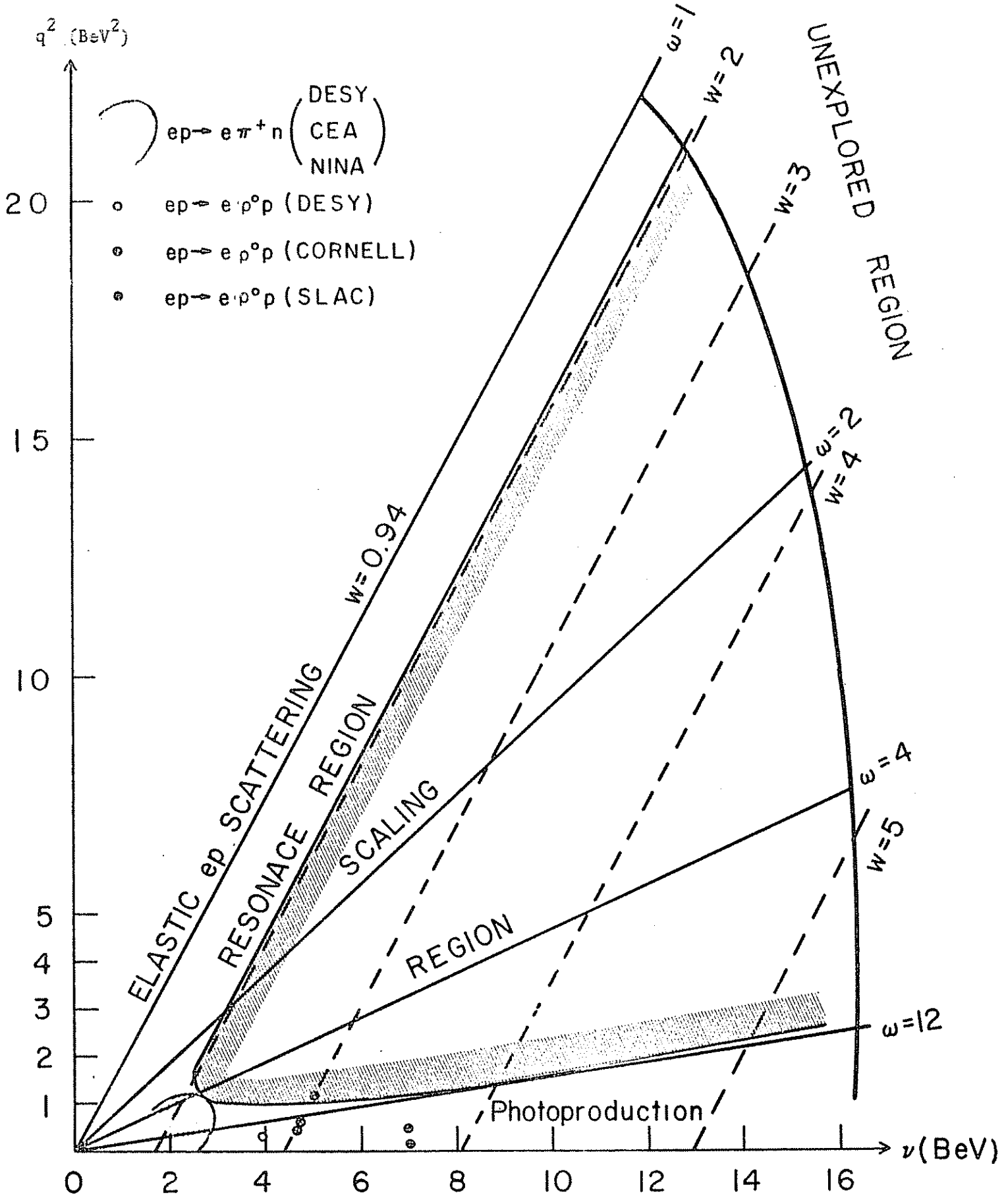
q^2 (BeV^2)
$ep \rightarrow e\pi^+ n$ (DESY, CEA, NINA)
$ep \rightarrow e\rho^0 p$ (DESY)
$ep \rightarrow e\rho^0 p$ (CORNELL)
$ep \rightarrow e\rho^0 p$ (SLAC)
ELASTIC ep SCATTERING
RESONACE REGION
SCALING REGION
UNEXPLORED REGION
W=0.94
W=2
W=3
W=4
W=5
ω=1
ω=2
ω=4
ω=12
Photoproduction
ν(BeV)
0
2
4
6
8
10
12
14
16
1
2
3
4
5
10
15
20

Fig. 1.

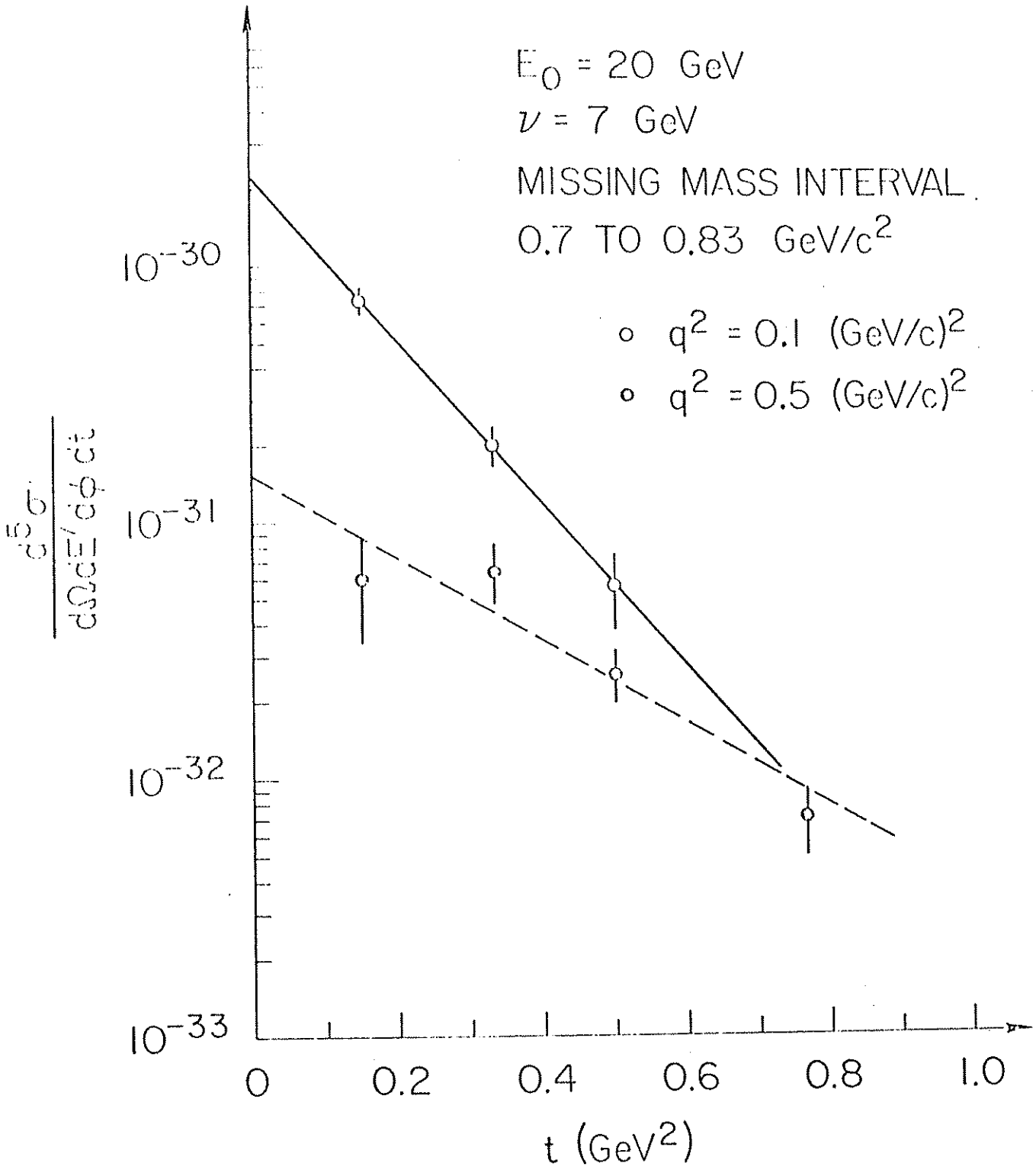
E_0 = 20 GeV
ν = 7 GeV
MISSING MASS INTERVAL
0.7 TO 0.83 GeV/c^2
o q^2 = 0.1 (GeV/c)^2
o q^2 = 0.5 (GeV/c)^2
10^{-30}
10^{-31}
10^{-32}
10^{-33}
$\frac{d\sigma}{dt}$ cm^2/GeV^2
0
0.2
0.4
0.6
0.8
1.0
t (GeV^2)

Fig. 2.

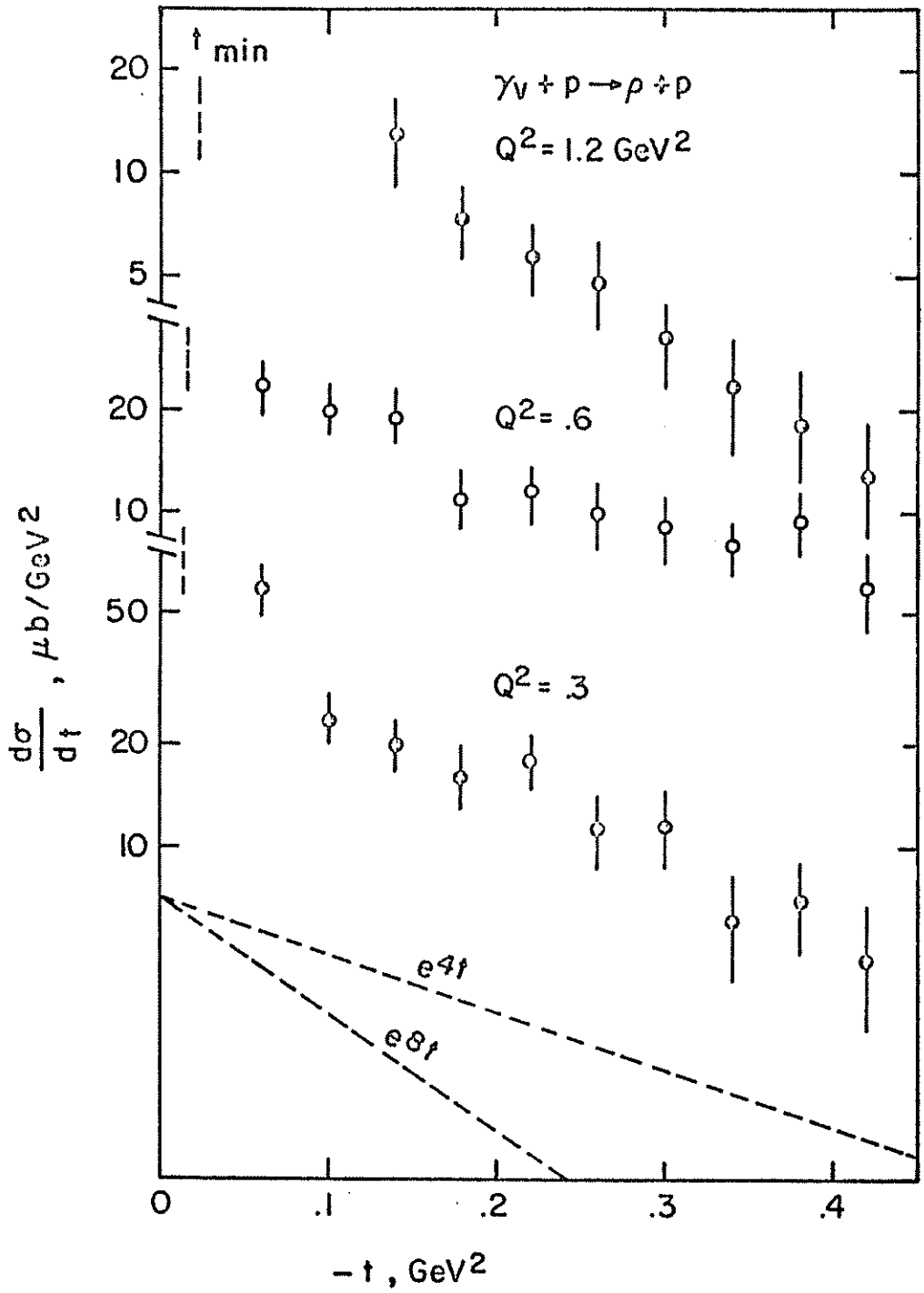
t min
$\gamma_V + p \rightarrow \rho + p$
$Q^2 = 1.2$ GeV^2
$Q^2 = .6$
$Q^2 = .3$
e^{4t}
e^{8t}
20
10
5
20
10
50
20
10
0
.1
.2
.3
.4
$\frac{d\sigma}{dt}$, μb/GeV^2
$-t$, GeV^2

Fig. 3.

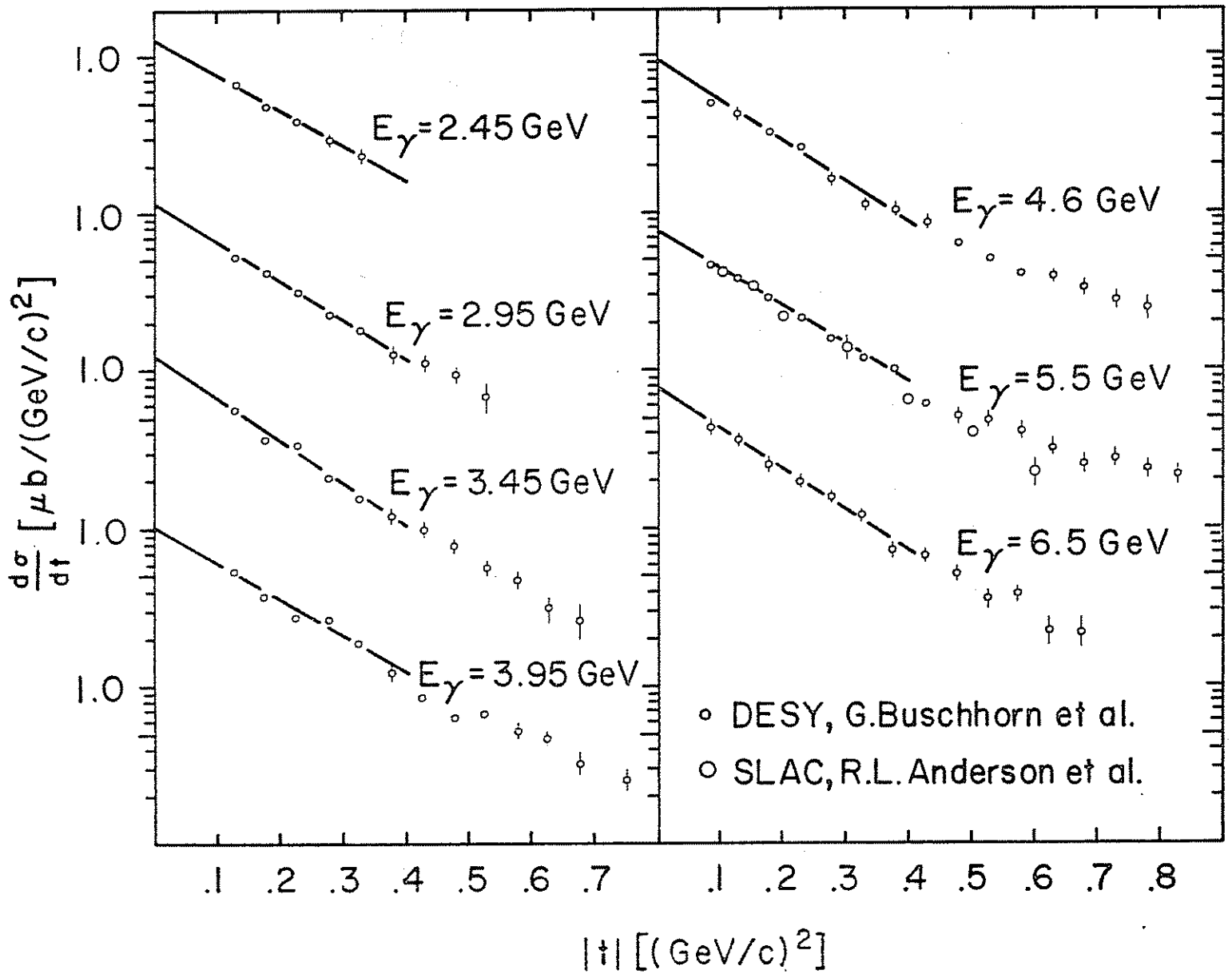
E_γ = 2.45 GeV
E_γ = 2.95 GeV
E_γ = 3.45 GeV
E_γ = 3.95 GeV
E_γ = 4.6 GeV
E_γ = 5.5 GeV
E_γ = 6.5 GeV
DESY, G.Buschhorn et al.
SLAC, R.L. Anderson et al.
$\frac{d\sigma}{dt}$ [μb/(GeV/c)^2]
|t| [(GeV/c)^2]
1.0
.1 .2 .3 .4 .5 .6 .7 .8

Fig. 4.

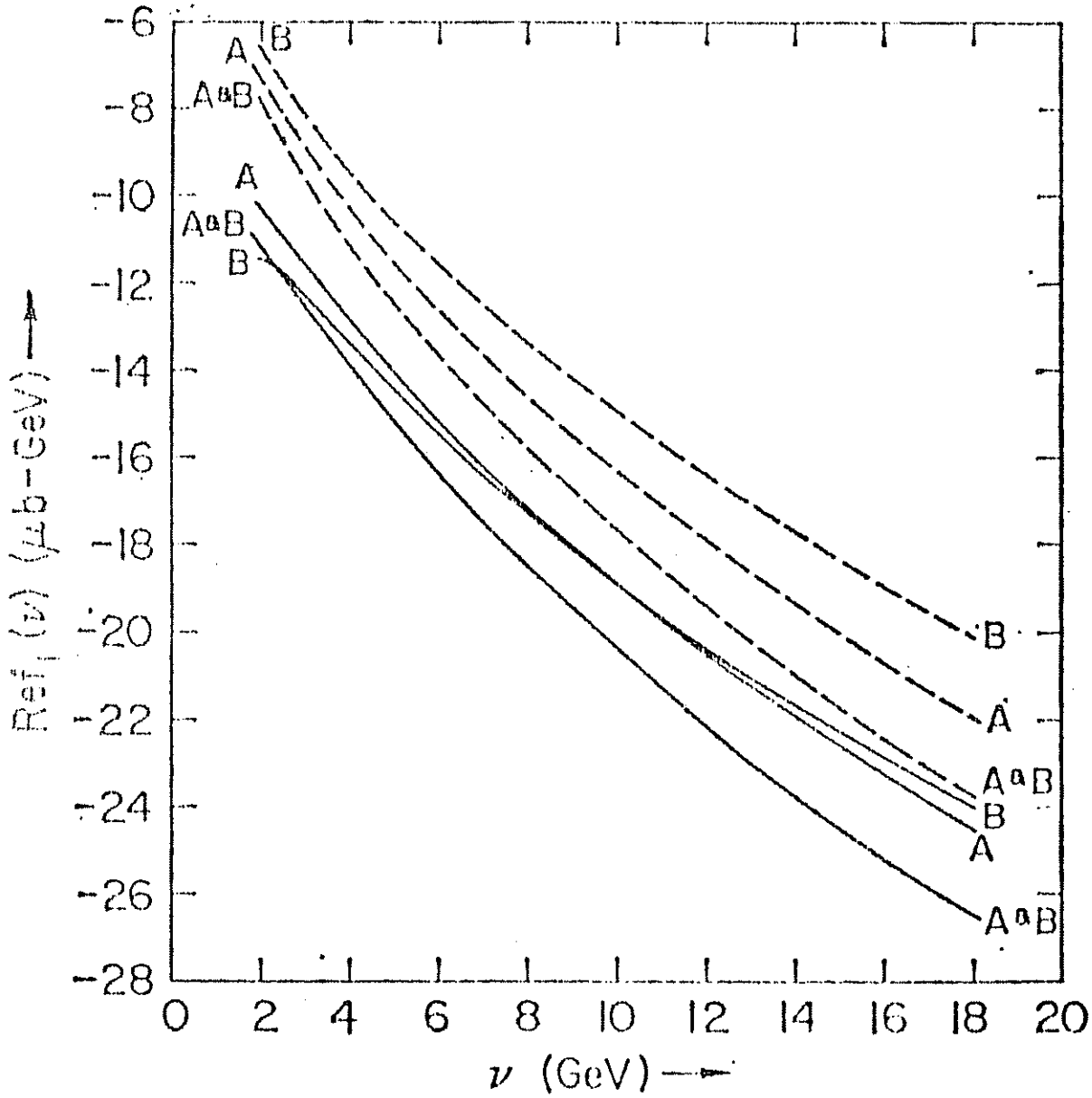
-6
-8
-10
-12
-14
-16
-18
-20
-22
-24
-26
-28
0
2
4
6
8
10
12
14
16
18
20
A
B
A∪B
A
A∪B
B
B
A
A∪B
B
A
A∪B
Re f1 (ν) (μb-GeV) ⟶
ν (GeV) ⟶

Fig. 5.

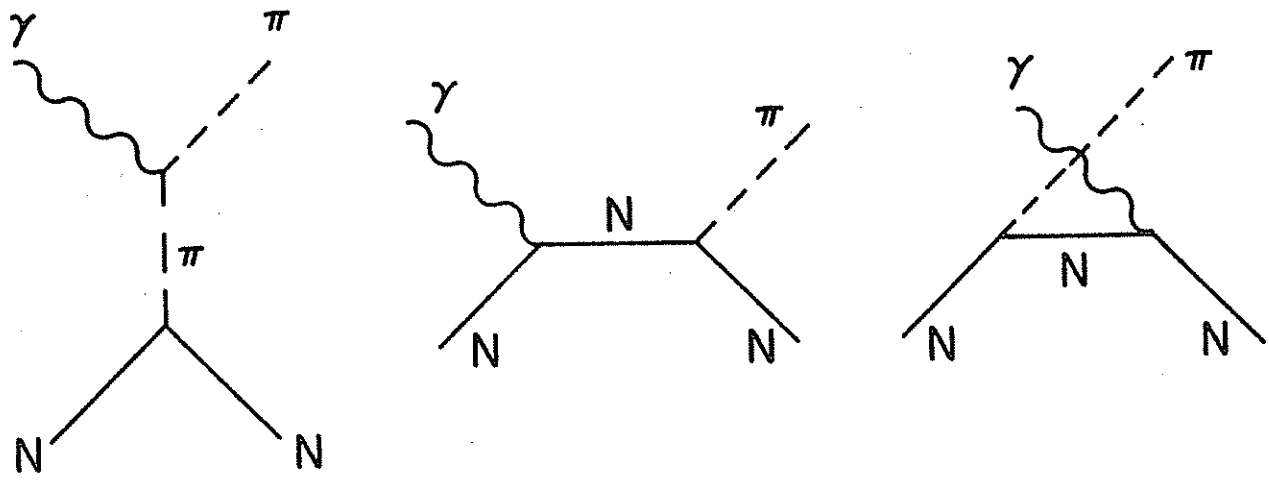

Fig. 6

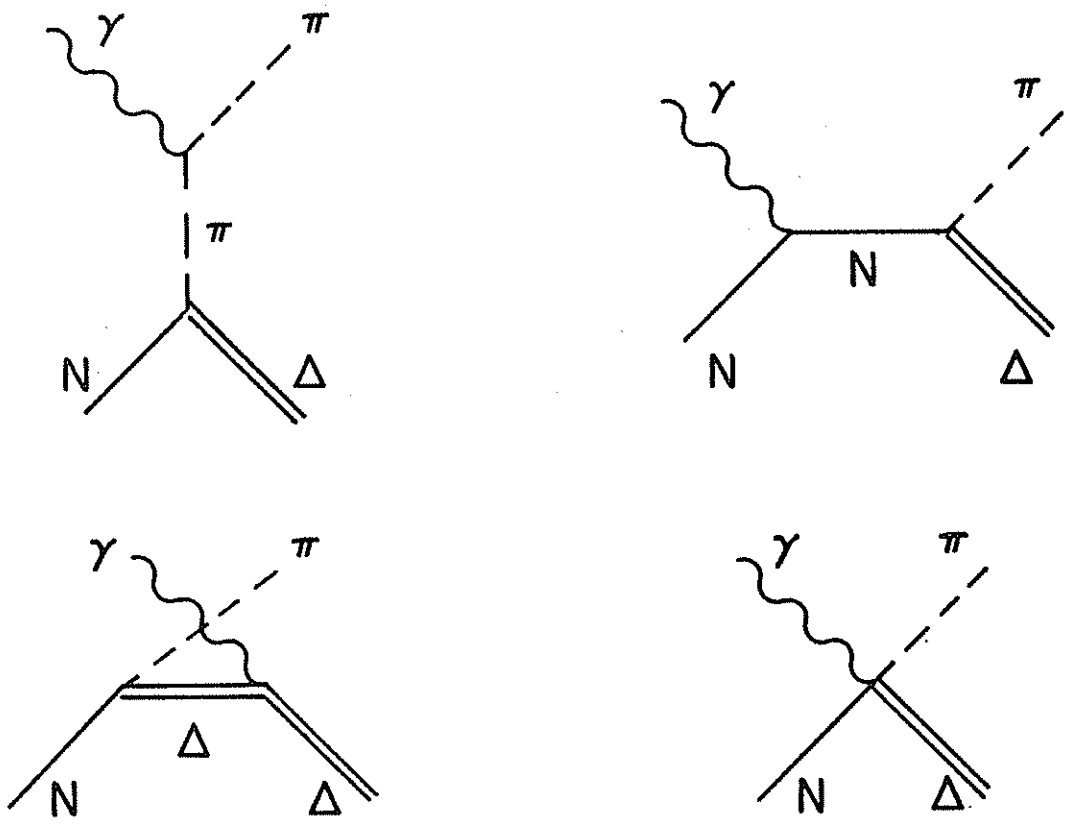

Fig. 7

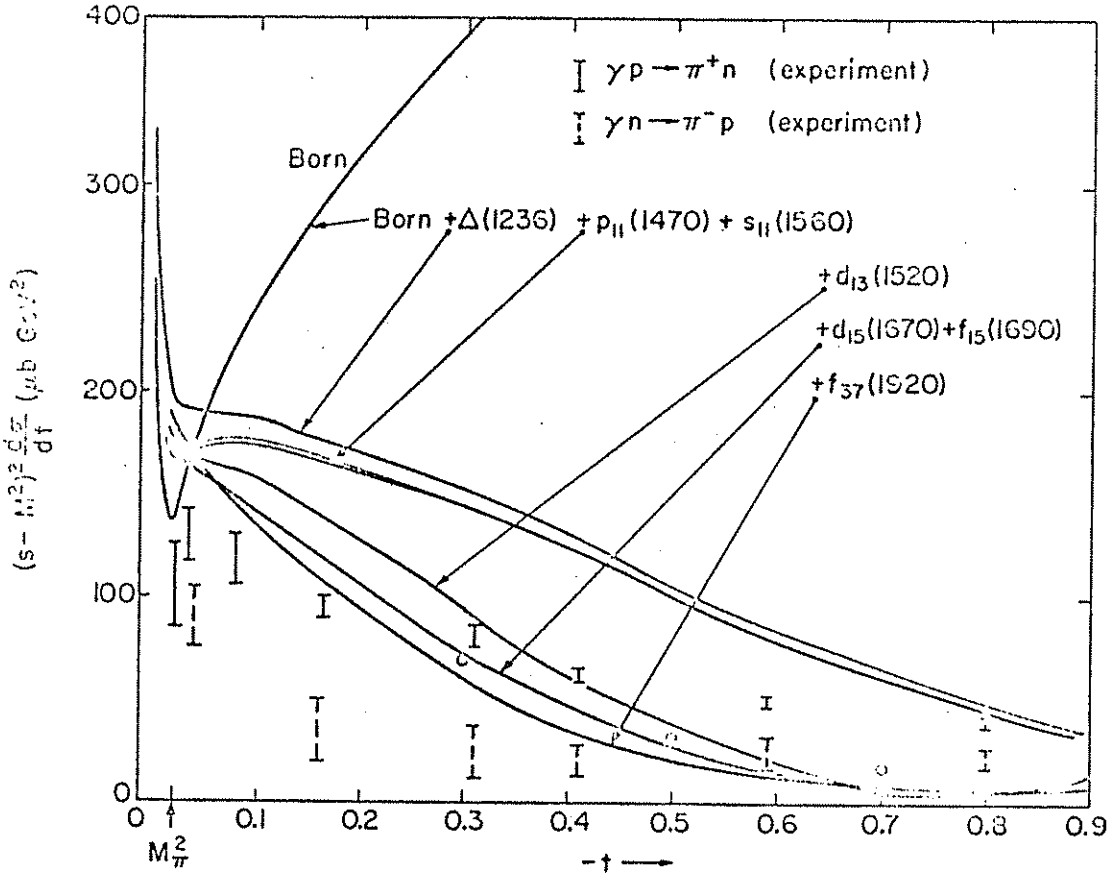
400
300
200
100
0
0
0.1
0.2
0.3
0.4
0.5
0.6
0.7
0.8
0.9
M_π^2
$-t \longrightarrow$
$\gamma p \to \pi^+ n$ (experiment)
$\gamma n \to \pi^- p$ (experiment)
Born
Born $+\Delta(1236)$ $+p_{11}(1470)+s_{11}(1560)$
$+d_{13}(1520)$
$+d_{15}(1670)+f_{15}(1690)$
$+f_{37}(1920)$

Fig. 8

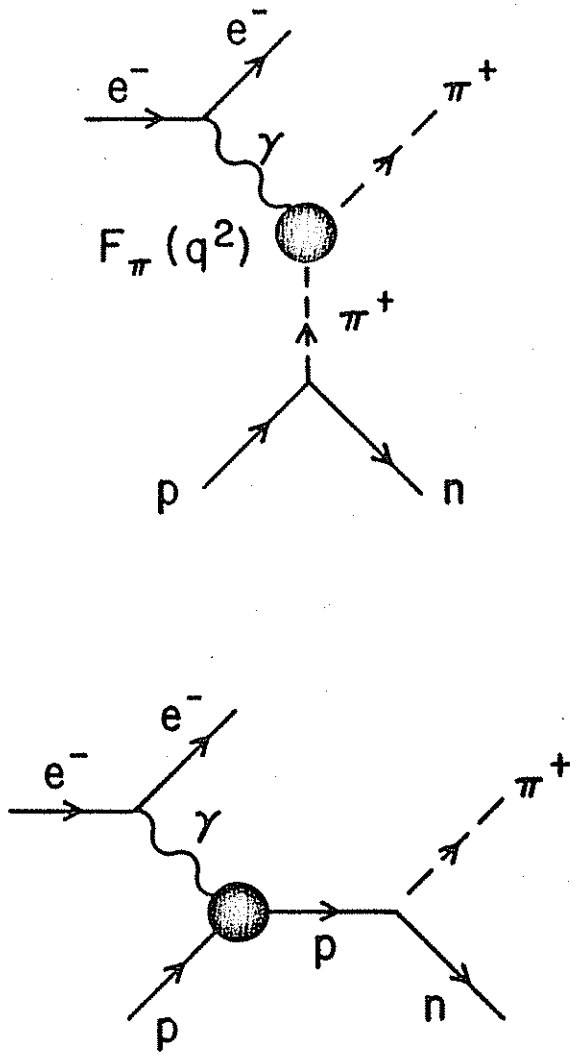

Fig. 9

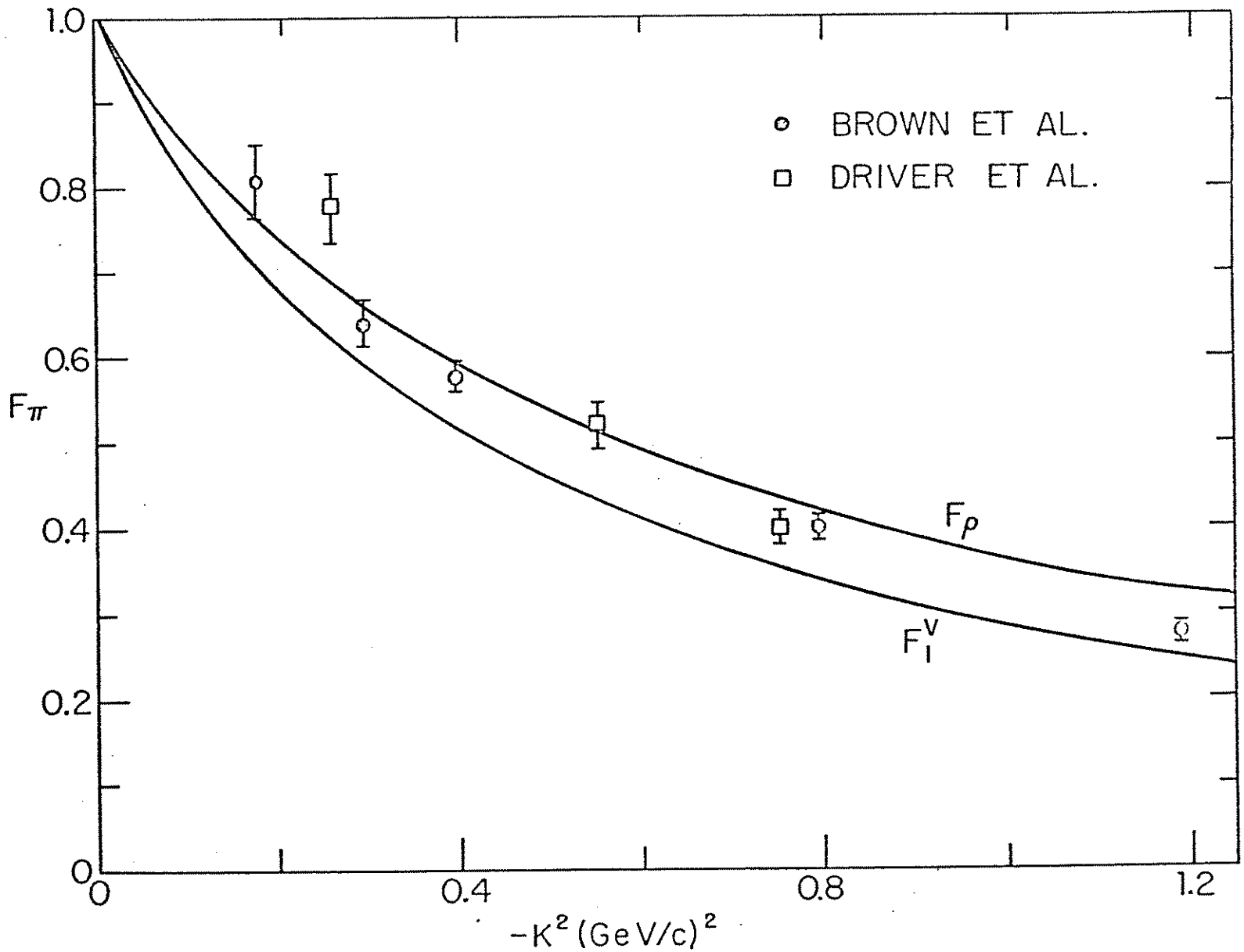
1.0
0.8
0.6
0.4
0.2
0
F_π
BROWN ET AL.
DRIVER ET AL.
F_ρ
F_1^V
0
0.4
0.8
1.2
$-K^2$ (GeV/c)^2

Fig. 10

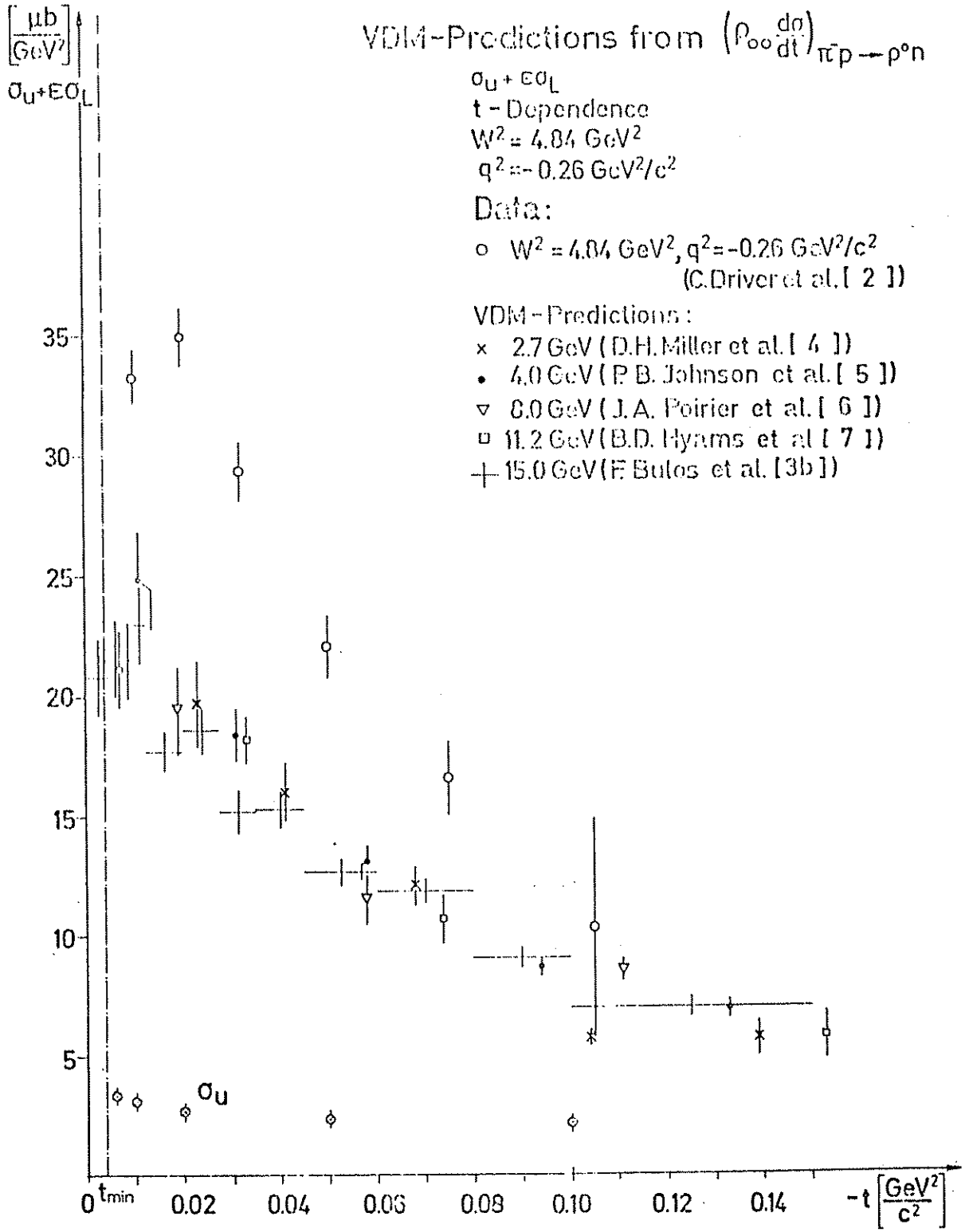
VDM-Predictions from $\left(\rho_{00}\frac{d\sigma}{dt}\right)_{\pi^- p \to \rho^0 n}$
$\sigma_u + \varepsilon\sigma_L$
t - Dependence
$W^2 = 4.84\ GeV^2$
$q^2 = -0.26\ GeV^2/c^2$
Data:
o $W^2 = 4.84\ GeV^2$, $q^2 = -0.26\ GeV^2/c^2$ (C.Driver et al. [2])
VDM-Predictions:
× 2.7 GeV (D.H.Miller et al. [4])
• 4.0 GeV (P.B. Johnson et al. [5])
▽ 8.0 GeV (J.A. Poirier et al. [6])
□ 11.2 GeV (B.D. Hyams et al [7])
+ 15.0 GeV (F.Bulos et al. [3b])
$\left[\frac{\mu b}{GeV^2}\right]$
$\sigma_u + \varepsilon\sigma_L$
35
30
25
20
15
10
5
σ_u
0
t_{min}
0.02
0.04
0.06
0.08
0.10
0.12
0.14
$-t\left[\frac{GeV^2}{c^2}\right]$

Fig. 11a

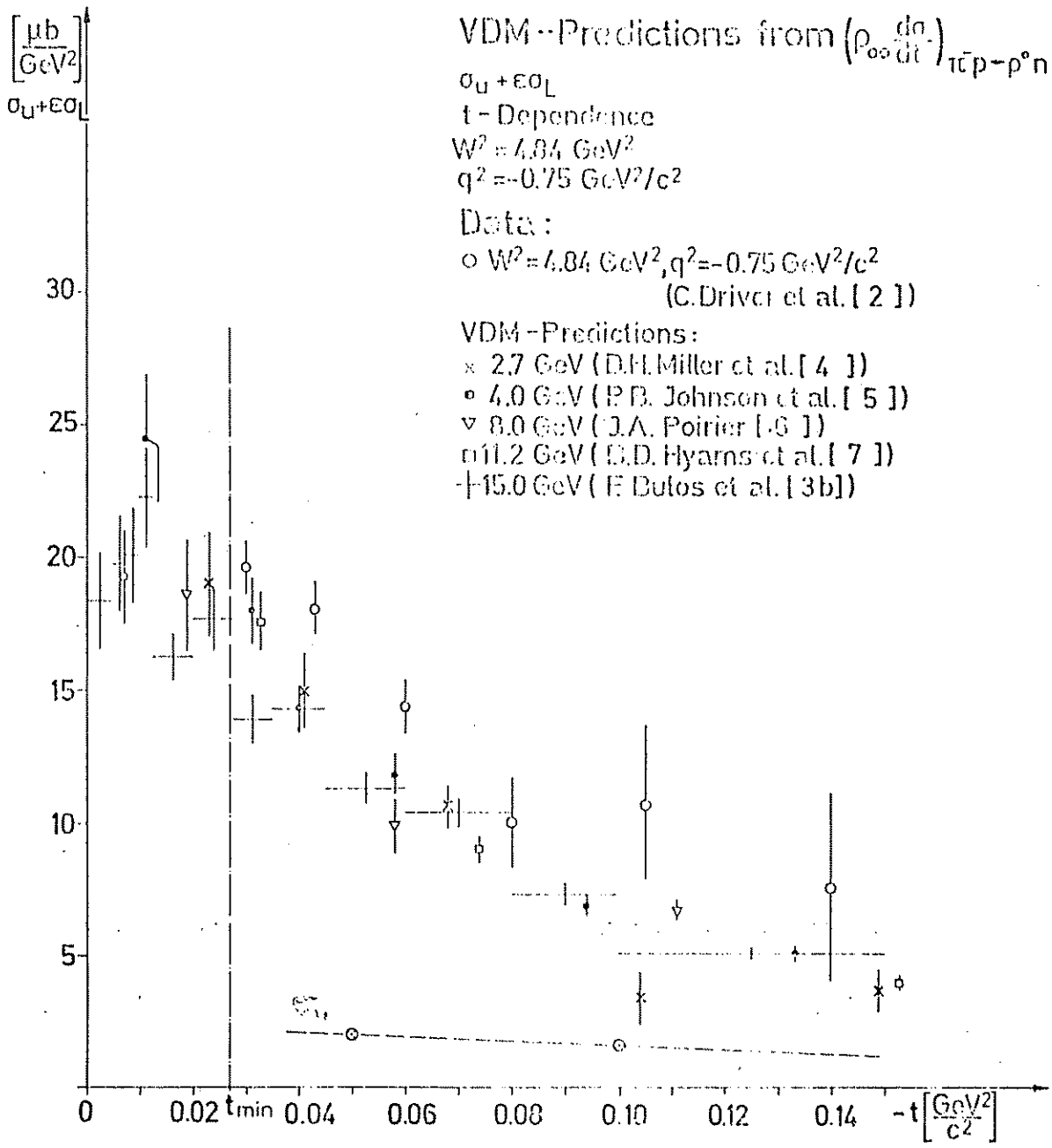
VDM--Predictions from $\left(\rho_{oo}\frac{d\sigma}{dt}\right)_{\pi^-p\to\rho^0n}$
$\sigma_u+\varepsilon\sigma_L$
t - Dependence
$W^2 = 4.84\ GeV^2$
$q^2 = -0.75\ GeV^2/c^2$
Data :
o $W^2=4.84\ GeV^2, q^2=-0.75\ GeV^2/c^2$ (C.Driver et al. [2])
VDM-Predictions:
× 2.7 GeV (D.H.Miller et al. [4])
• 4.0 GeV (P.B. Johnson et al. [5])
▽ 8.0 GeV (J.A. Poirier [6])
□ 11.2 GeV (B.D. Hyams et al. [7])
+ 15.0 GeV (F. Dutos et al. [3b])
$\left[\frac{\mu b}{GeV^2}\right]$
$\sigma_u+\varepsilon\sigma_L$
30
25
20
15
10
5
0
0.02
t_{min}
0.04
0.06
0.08
0.10
0.12
0.14
$-t\left[\frac{GeV^2}{c^2}\right]$

Fig. 11b

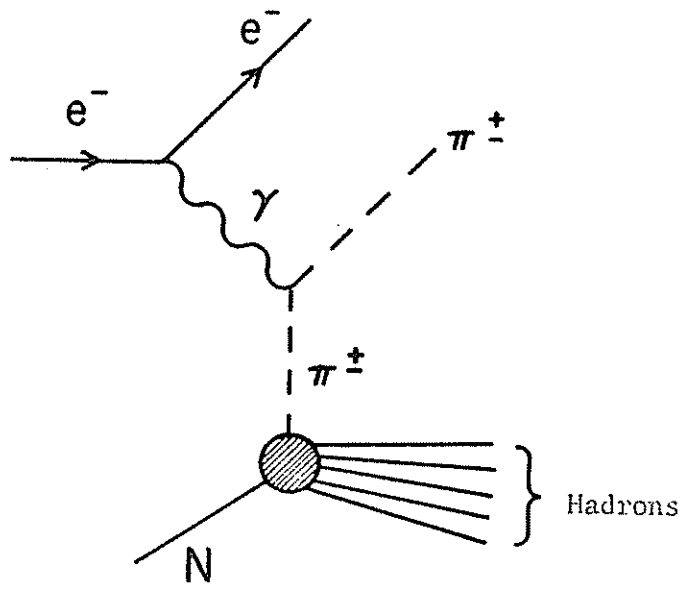

Fig. 12

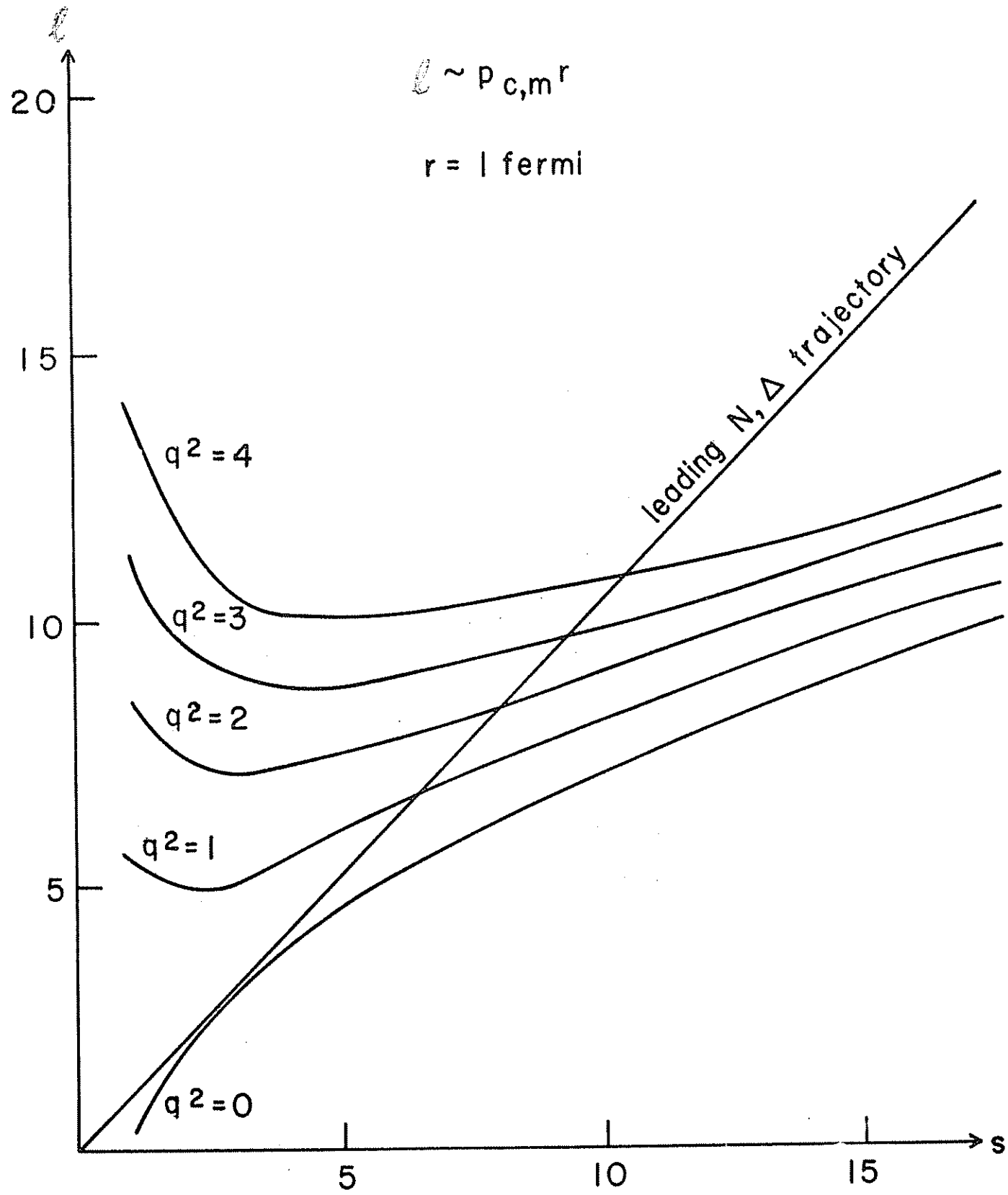
ℓ
ℓ ~ p c,m r
r = 1 fermi
20
15
10
5
q² = 4
q² = 3
q² = 2
q² = 1
q² = 0
leading N, Δ trajectory
5
10
15
s

Fig. 13

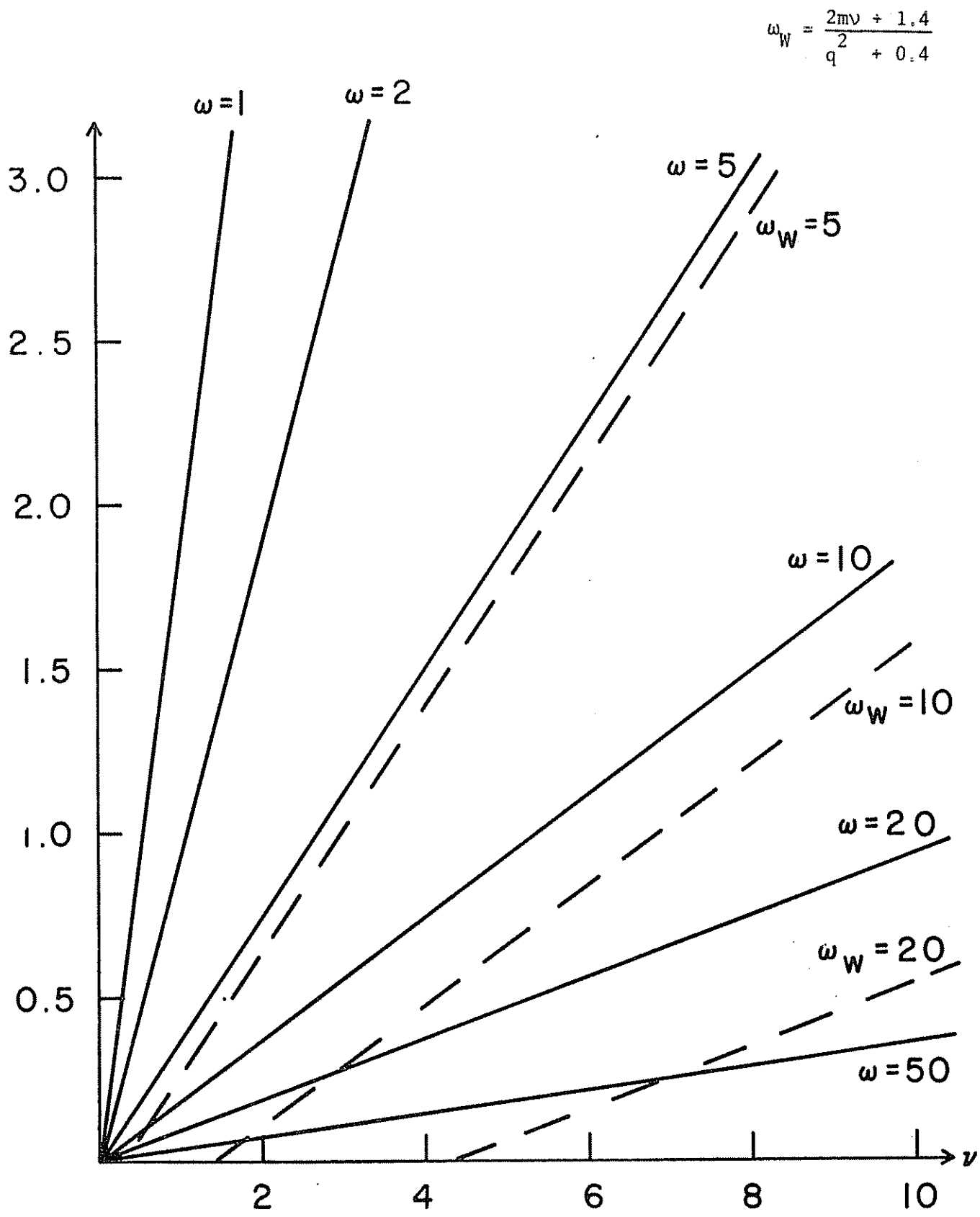
$\omega_W = \frac{2m\nu + 1.4}{q^2 + 0.4}$
ω = 1
ω = 2
ω = 5
ω_W = 5
ω = 10
ω_W = 10
ω = 20
ω_W = 20
ω = 50
3.0
2.5
2.0
1.5
1.0
0.5
2
4
6
8
10
ν

Fig. 14